^{187}Re–^{187}Os geochronology of Precambrian organic-rich sedimentary rocks

BRIAN KENDALL[1,2]*, ROBERT A. CREASER[2] & DAVID SELBY[3]

[1]*School of Earth and Space Exploration, Arizona State University, Tempe, AZ 85287-1404, USA*

[2]*Department of Earth and Atmospheric Sciences, University of Alberta, Edmonton, Alberta, Canada T6G 2E3*

[3]*Department of Earth Sciences, Science Labs, University of Durham, Durham DH1 3LE, UK*

**Corresponding author (e-mail: brian.kendall@asu.edu)*

Abstract: Global correlations of Precambrian stratigraphic successions can be hampered by the coarse resolution of biostratigraphic and chemostratigraphic records, and by the scarcity of reliable U–Pb zircon age constraints. The development of the ^{187}Re (rhenium)–^{187}Os (osmium) radioisotope system as an accurate deposition-age geochronometer for organic-rich sedimentary rocks (e.g. black shales) holds great potential for an improved radiometric calibration of the Precambrian rock record. Here, we review Re–Os isotope data obtained for Precambrian black shales and revisit the discrepancy in Re–Os ages for the Neoproterozoic Aralka Formation (central Australia). In addition, we introduce new Re–Os isotope data for the Late Neoproterozoic Doushantuo Formation (South China) that highlights the necessity of a rigorous sampling protocol for depositional age determinations. Improvements in sampling and analytical methodologies have permitted the determination of precise ages ($<1\%$, 2σ) from Late Neoproterozoic to Late Archaean shales. Whole-rock digestion using a Cr^{VI}–H_2SO_4 solution minimizes the release of detrital Re and Os from shale matrices, and selectively attacks organic matter that hosts hydrogenous Re and Os. The Re–Os system in organic-rich sedimentary rocks appears to be robust during hydrocarbon maturation and up to the onset of lowermost greenschist facies metamorphism, but post-depositional hydrothermal fluid flow can result in scattered Re–Os isotope data. The Re–Os black shale geochronometer should find utility for constraining the age of a diverse range of Precambrian geological phenomena. In addition, the initial $^{187}Os/^{188}Os$ composition determined from Re–Os isochron regressions serves as a tracer for the Os isotope composition of Precambrian sea water.

Accurately determining the depositional ages of sedimentary rocks has proven extremely difficult to accomplish using the conventional long-lived radioisotope systems (e.g. Rb–Sr, Sm–Nd, U–Pb, K–Ar). The U–Pb SHRIMP (sensitive high-resolution ion microprobe) dating of detrital minerals such as zircon has proven useful for provenance studies and constraining the maximum depositional age (e.g. Bingen *et al.* 2005). However, authigenic minerals (e.g. apatite, glauconite, illite, K-feldspar, monazite) generally yield diagenetic ages that are variably younger than the depositional age of the host sedimentary rock. Diagenetic age determinations on authigenic minerals are also hampered by low closure temperatures of the applied radioisotope system, resulting in a high susceptibility to thermal resetting even during relatively low-temperature hydrothermal alteration or metamorphism (Dickin 2005). Diagenetic xenotime is found in a wide variety of siliciclastic and volcaniclastic rocks, and represents a robust U–Pb geochronometer with the potential for resolving complex geological histories within sedimentary basins (Rasmussen 2005). However, U–Pb xenotime dates also reflect the timing of diagenesis rather than deposition. In some cases, Pb/Pb ages from carbonates (e.g. Moorbath *et al.* 1987; Woodhead *et al.* 1998; Babinski *et al.* 2007) and phosphorites (Barfod *et al.* 2002; Chen *et al.* 2004) may yield depositional or early diagenetic ages using well-preserved material. However, Pb/Pb ages may be erroneously young or old owing to diagenetic or metamorphic recrystallization and detrital inheritance, respectively, or age information may be lost altogether due to post-depositional mobility of U and Pb (Rasmussen 2005).

Currently, the most reliable method of constraining the depositional age of sedimentary rocks is by U–Pb zircon dating of interbedded tuff horizons. In the case of Phanerozoic sedimentary basins, such U–Pb ages can be used to calibrate high-resolution Phanerozoic biostratigraphic, chemostratigraphic and magnetostratigraphic records, thereby facilitating regional and global correlations of stratigraphic successions (e.g. Gradstein *et al.* 2004). However, the generally coarse resolution of these

From: CRAIG, J., THUROW, J., THUSU, B., WHITHAM, A. & ABUTARRUMA, Y. (eds) *Global Neoproterozoic Petroleum Systems: The Emerging Potential in North Africa.* Geological Society, London, Special Publications, **326**, 85–107.
DOI: 10.1144/SP326.5 0305-8719/09/$15.00

chronostratigraphic methods for the Precambrian rock record does not currently permit this approach, and, in cases where datable ash beds are absent, the ages of Precambrian sedimentary rocks are generally only poorly constrained by radiometric dates from overlying and underlying volcanic or plutonic rocks, and/or cross-cutting plutonic rocks.

The development of the $^{187}Re-^{187}Os$ radioisotope system as a reliable deposition-age geochronometer for organic-rich sedimentary rocks (ORS; total organic carbon (TOC) $\geq$0.5%) like black shales (Ravizza & Turekian 1989; Cohen *et al.* 1999; Creaser *et al.* 2002; Selby & Creaser 2003; Kendall *et al.* 2004) has the potential to alleviate the problems associated with radiometric calibration of the Precambrian sedimentary rock record. Improvements in sampling and analytical methodologies, combined with the high precision of isotope dilution–negative thermal ionization mass spectrometry (ID-NTIMS: Creaser *et al.* 1991; Völkening *et al.* 1991; Walczyk *et al.* 1991), have made it possible to obtain a Re–Os age for black shale with a precision of better than $\pm$1% (2σ), with the absolute uncertainty comparable in some cases to the uncertainties on U–Pb ages derived from SHRIMP or laser ablation MC-ICP-MS (multicollector-inductively coupled plasma-mass spectrometry) analyses of zircons from tuffaceous beds (e.g. Kendall *et al.* 2004, 2006; Selby & Creaser 2005*a*; Anbar *et al.* 2007; Creaser & Stasiuk 2007).

Recently, the Re–Os ORS geochronometer has been successfully applied to studies regarding geological timescale calibration (Devonian–Mississippian boundary: Selby & Creaser 2005*a*), the timing of Proterozoic glaciation (Hannah *et al.* 2004; Kendall *et al.* 2004, 2006; Azmy *et al.* 2008), the Earth's early history of atmosphere and ocean oxygenation (Hannah *et al.* 2004; Anbar *et al.* 2007), and sedimentary basin analysis (Hannah *et al.* 2006; Creaser & Stasiuk 2007; Kendall *et al.* 2009*a*). In addition, the initial $^{187}Os/^{188}Os$ value (I_{Os}) from Re–Os isochron regressions has served as a tracer for the Os isotope composition of Phanerozoic sea water (Cohen *et al.* 1999, 2004; Creaser *et al.* 2002; Selby & Creaser 2003; Cohen 2004; Cohen & Coe 2007; Selby 2007). Here, we review recent applications of Re–Os geochronology to Precambrian ORS, and demonstrate how careful sampling and analytical methodologies are essential for precise and accurate depositional age determinations.

The $^{187}Re-^{187}Os$ system in ORS: a deposition-age geochronometer and sea-water Os isotope tracer

In addition to being siderophilic and chalcophilic (e.g. Shirey & Walker 1998), Re and Os are also organophilic and redox-sensitive (Ravizza *et al.* 1991; Ravizza & Turekian 1992; Colodner *et al.* 1993; Crusius *et al.* 1996; Levasseur *et al.* 1998; Selby & Creaser 2003, 2005*b*; Selby *et al.* 2005, 2007*a*). This geochemical behaviour of Re and Os in Earth surface environments enables the $^{187}Re-^{187}Os$ isotope system to be used as a deposition-age geochronometer for ORS and a tracer of palaeo-sea-water Os isotope composition.

Under oxidizing atmospheric conditions, Re is transported to the oceans primarily by rivers (as the highly soluble perrhenate anion ReO_4^-: Colodner *et al.* 1993). Rhenium is removed rapidly from reducing pore waters at centimetres to tens of centimetres below the sediment–water interface, and is sequestered into suboxic, anoxic and euxinic sediments (Colodner *et al.* 1993; Crusius *et al.* 1996; Morford & Emerson 1999; Nameroff *et al.* 2002; Sundby *et al.* 2004; Morford *et al.* 2005). Removal of Re from pore waters occurs by reductive capture ($Re^{VII}O_4^-$ is reduced to Re^{IV}: Colodner *et al.* 1993), the rate of which is controlled by slow precipitation kinetics (Crusius & Thomson 2000; Sundby *et al.* 2004).

The $^{187}Os/^{188}Os$ isotopic composition of present-day sea water is almost homogenous (*c.* 1.06: Sharma *et al.* 1997; Levasseur *et al.* 1998; Burton *et al.* 1999; Woodhouse *et al.* 1999; Peucker-Ehrenbrink & Ravizza 2000), consistent with an Os sea-water residence time of approximately 10^4 years (Oxburgh 1998, 2001; Levasseur *et al.* 1999). The dominant source of present-day sea-water Os (*c.* 70–80%) is from the weathering of the upper continental crust (McDaniel *et al.* 2004). Average $^{187}Os/^{188}Os$ for the currently eroding upper continental crust and riverine inputs are between 1.0 and 1.4 (Esser & Turekian 1993; Peucker-Ehrenbrink & Jahn 2001; Hattori *et al.* 2003) and approximately 1.5 (with an uncertainty of >20%: Levasseur *et al.* 1999), respectively. The remainder of the present-day marine Os budget is derived from extraterrestrial cosmic dust (Peucker-Ehrenbrink 1996) and the low- and high-temperature hydrothermal alteration of oceanic crust and peridotites (Ravizza *et al.* 1996; Sharma *et al.* 2000, 2007; Cave *et al.* 2003). Both sources contribute unradiogenic $^{187}Os/^{188}Os$ to sea water (0.126–0.130: Becker *et al.* 2001; Meisel *et al.* 1996, 2001; Walker *et al.* 2002*a*, *b*). Dissolved Os is probably present in sea water as an octavalent oxyanion (e.g. $HOsO_5^-$, $H_3OsO_6^-$). Osmium is removed into organic-rich sediments in direct association with organic matter (Levasseur *et al.* 1998) and/or is rapidly removed to organic-rich sediments first as Os (IV), and then is further reduced to Os (III) by organic complexation (Yamashita *et al.* 2007). Osmium removal from sea water into reducing sediments may occur below the depth of Re enrichment (Poirer 2006).

Rhenium and Os in ORS are predominantly hydrogenous, and are physically associated with organic matter (Ravizza & Turekian 1989, 1992; Ravizza *et al.* 1991; Ravizza & Esser 1993; Cohen *et al.* 1999; Martin *et al.* 2000; Peucker-Ehrenbrink & Hannigan 2000; Pierson-Wickmann *et al.* 2000, 2002; Creaser *et al.* 2002; Jaffe *et al.* 2002). Rhenium and Os are present in natural hydrocarbons (Poplavko *et al.* 1975; Barre *et al.* 1995; Woodland *et al.* 2001; Selby & Creaser 2005*b*; Selby *et al.* 2007*a*) and bitumens (Selby *et al.* 2005), and bulk organic matter is known to contain a large fraction of the Re and Os in shale source rocks (Ripley *et al.* 2001; Selby & Creaser 2003).

The fundamental assumptions behind the Re–Os ORS geochronometer include: (1) a hydrogenous origin for all Re and Os in ORS (i.e. negligible contributions from detrital and/or extraterrestrial particulates); (2) the closed-system behaviour of Re and Os in ORS following sediment deposition, such that Re–Os dates reflect the timing of deposition rather than diagenesis; (3) a homogenous I_{Os} derived from the contemporaneous sea water; and (4) the negligible post-depositional mobilization of Re and Os. Obtaining a precise Re–Os age by the isochron method requires a suitable range in initial $^{187}Re/^{188}Os$ such that β-decay of ^{187}Re to ^{187}Os over time generates a range in present-day $^{187}Os/^{188}Os$. Although ORS may contain Re and Os concentrations ranging from average upper-crustal abundances (*c.* 0.2–2 ppb Re and 30–50 ppt Os: Esser & Turekian 1993; Peucker-Ehrenbrink & Jahn 2001; Hattori *et al.* 2003; Sun *et al.* 2003*a*, *b*) to hundreds of ppb Re and several ppb Os (e.g. Cohen *et al.* 1999), the high Re/Os ratios of ORS derived from sea water (present-day sea-water $^{187}Re/^{188}Os$ ratio is *c.* 3200–5300) means that only moderate enrichments in Re are required to generate radiogenic present-day $^{187}Os/^{188}Os$ ratios for Precambrian ORS (e.g. Kendall *et al.* 2004, 2006). One significant challenge of Re–Os ORS geochronology concerns the first assumption, which requires an analytical methodology to release hydrogenous Os from shales while minimizing release of detrital Re and Os that could otherwise affect the accuracy and precision of Re–Os age and I_{Os} determinations (e.g. Ravizza *et al.* 1991). Extraterrestrial material can be a negligible source of Os to ORS (e.g. <0.2% of total Os for ORS, with Os abundances >150 ppt, sediment accumulation rates >50 m Ma^{-1} and meteoritic fluxes comparable to Cenozoic fluxes) (Cohen *et al.* 1999; Kendall *et al.* 2004).

Development of the Re–Os geochronometer for ORS

The development of Re–Os ORS geochronology resulted from several studies on Phanerozoic shales. Using the NiS fire assay for preconcentration of Re and Os (and acid dissolution for Re in some samples), and isotope dilution-secondary ion mass spectrometry (ID-SIMS), Ravizza & Turekian (1989) obtained Re–Os isotope data for the upper Mississippian Bakken Shale (North Dakota, USA). Regression of their data using Isoplot V. 3.0 (Ludwig 2003) and the value of 1.666×10^{-11} $year^{-1}$ for $\lambda^{187}Re$ (Smoliar *et al.* 1996; Selby *et al.* 2007*b*) yields a Re–Os age of 323 $\pm$ 110 Ma (2σ, Model 3, mean square of weighted deviates (MSWD) = 5.6) that is broadly consistent with known biostratigraphic age constraints (*c.* 360–352 Ma) for the Bakken Shale. The large uncertainty in the Re–Os date reflects in part the poor precision (3–10%) of $^{187}Os/^{186}Os$ ratios measured by SIMS (Luck & Allègre 1983). Ravizza & Turekian (1989) suggested that some of the scatter about the regression line resulted predominantly from disturbance of the Re–Os systematics by hydrocarbon maturation.

Using new analytical methodologies, including the Carius tube technique for whole-rock digestions in inverse aqua regia (Shirey & Walker 1995), improved chemical separation and purification protocols for Os (Cohen & Waters 1996) and ID-NTIMS analysis, Cohen *et al.* (1999) provided the first relatively precise Re–Os age determinations from hydrocarbon immature, high-TOC (>5%), Jurassic ORS from the UK. Cohen *et al.* (1999) obtained Re–Os ages of 207 $\pm$ 12 Ma (Model 3, MSWD = 88), 181 $\pm$ 13 Ma (Model 3, MSWD = 17) and 155.2 $\pm$ 4.3 Ma (Model 3, MSWD = 11) for Hettangian (Blue Lias, Dorset), Toarcian (Jet Rock, Yorkshire) and Kimmeridgian (Kimmeridge Clay, Dorset) shales. These ages agree within uncertainty to the respective stratigraphic ages of 198.0 $\pm$ 1.5, 179.3 $\pm$ 3.7 and 152.7 $\pm$ 1.9 Ma (Gradstein *et al.* 2004). Cohen *et al.* (1999) established that sampling of stratigraphic intervals representing short intervals of geological time were required to minimize I_{Os} heterogeneity and obtain precise Re–Os depositional ages. Cohen *et al.* (1999) also considered the selection of immature ORS, which have not undergone hydrocarbon maturation, as a necessary sampling protocol for precise and accurate Re–Os geochronology. However, Creaser *et al.* (2002) found that regression of hydrocarbon immature, mature and overmature samples gave a Re–Os age of 358 $\pm$ 10 Ma (Model 3, MSWD = 19) for the Late Devonian Exshaw Formation (Western Canada Sedimentary Basin) lower black shale member. The Re–Os age is consistent with a previous U–Pb monazite age (363.3 $\pm$ 0.4 Ma) from a tuff at the base of the lower black shale member (Richards *et al.* 2002). Individual regressions for immature and mature plus overmature samples

yield statistically indistinguishable Re–Os dates (at 2σ uncertainties) and thus hydrocarbon maturation did not grossly perturb the Re–Os system in this ORS. Further, Creaser *et al.* (2002) showed that non-hydrogenous Re and Os can be liberated by inverse aqua regia whole-rock digestions, and thus negatively impact the precision and accuracy of Re–Os ages derived from low-TOC samples.

To limit the release of detrital Re and Os from ORS matrices, a new whole-rock digestion protocol (using a Cr^{VI}–H_2SO_4 solution) was developed by Selby & Creaser (2003). Using the same Exshaw Formation shale aliquots as Creaser *et al.* (2002), two subsets with distinctive $I_{Os(364\,Ma)}$ values were identified and separately regressed to yield Re–Os ages of 366.1 ± 9.6 Ma (Model 3, MSWD = 2.2; $I_{Os} = 0.51 \pm 0.06$) and 363.4 ± 5.6 Ma (Model 1, MSWD = 1.6; $I_{Os} = 0.41 \pm 0.04$). These Re–Os ages are more precise and better correlated than the Re–Os ages for the same subsets derived using the data from Creaser *et al.* (2002) for inverse aqua regia digestion (356 ± 23 Ma, MSWD = 11.1; and 356 ± 12 Ma, MSWD = 5.2). Selby & Creaser (2003) thus showed that the Cr^{VI}–H_2SO_4 medium represents a superior digestion protocol to inverse aqua regia for obtaining depositional ages and the $^{187}Os/^{188}Os$ isotope composition of contemporaneous sea water. Similarly, Kendall *et al.* (2004) obtained an imprecise Re–Os age of 634 ± 57 Ma (Model 3, MSWD = 65) with inverse aqua regia digestion, but a precise age of 607.8 ± 4.7 Ma (Model 1, MSWD = 1.2) was obtained using Cr^{VI}–H_2SO_4 digestion of the same shale powders of low-TOC (<1%) slates from the Late Neoproterozoic Old Fort Point Formation, Windermere Supergroup, Western Canada (Fig. 1). The 607.8 ± 4.7 Ma age agrees with existing Windermere Supergroup U–Pb age constraints that bracket the Old Fort Point Formation to between approximately 700–667 and 570 Ma (Colpron *et al.* 2002; Lund *et al.* 2003; Fanning & Link 2004, 2008). Neither chlorite-grade metamorphism nor low-TOC content precluded a precise Re–Os age determination (using Cr^{VI}–H_2SO_4 digestion) for the Old Fort Point Formation.

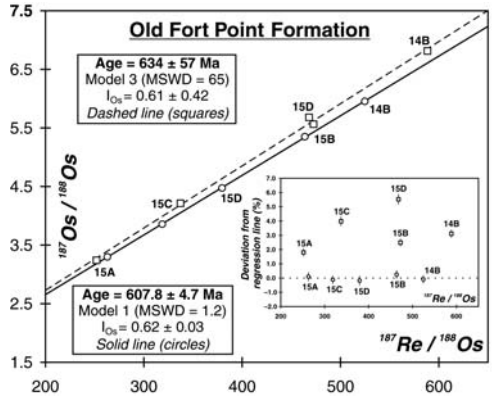

Fig. 1. Re–Os isochron diagram for the Neoproterozoic Old Fort Point Formation, Windermere Supergroup, Western Canada (Kendall *et al.* 2004). Regression of inverse aqua regia analyses (squares, dashed regression line) yields an imprecise Model 3 age, whereas regression of Cr^{VI}–H_2SO_4 digestion analyses (circles, solid regression line) yields a precise Model 1 age. The inset diagram shows the deviation of each point from the Cr^{VI}–H_2SO_4 best-fit regression line. Regression used measured 2σ uncertainties for both $^{187}Re/^{188}Os$ and $^{187}Os/^{188}Os$, and, for the first time, the error correlation function (ρ) (Ludwig 1980). Use of the latter is justified by generally significant error correlations between $^{187}Re/^{188}Os$ and $^{187}Os/^{188}Os$ (*c.* 0.4–0.6 in this case).

Accuracy of the Re–Os geochronometer for ORS and the ^{187}Re decay constant

An accurate and precise determination of the ^{187}Re decay constant, together with agreement between Re–Os black shale and U–Pb zircon ages from the same rock unit, are necessary prerequisites to qualify the Re–Os system as an accurate deposition-age geochronometer for ORS. The most widely used value of $\lambda^{187}Re$ ($1.666 \pm 0.005 \times 10^{-11}$ year^{-1}), determined by Smoliar *et al.* (1996), was calculated using the slope of Re–Os data from group IIIA iron meteorites and the Pb/Pb age of 4557.8 ± 0.4 Ma determined for angrite meteorites (Lugmair & Galer 1992) that are assumed to form at the same time as group IIIA irons. This assumption is supported by ^{53}Mn–^{53}Cr ages for angrite and group IIIAB meteorites that constrain their formation to be within ±5 Ma of each other (Hutcheon & Olsen 1991; Hutcheon *et al.* 1992). Although the uncertainty in $\lambda^{187}Re$ was calculated to be ±0.31% (2σ) by Smoliar *et al.* (1996), the ammonium hexachloro-osmate standard used by these researchers is only stoichiometric to within ±1.2% (Morgan *et al.* 1995) and thus the total uncertainty in $\lambda^{187}Re$ would be approximately 1% (2σ) for spike solutions not calibrated against the particular Os standard used by Smoliar *et al.* (1996). Subsequent studies have yielded slightly different values for $\lambda^{187}Re$ using either direct counting experiments or analyses from meteorites (Shukolyukov & Lugmair 1997; Birck & Allègre 1998; Shen *et al.* 1998). Recently, Selby *et al.* (2007*b*) intercalibrated the Re–Os molybdenite and U–Pb zircon chronometres using 11 magmatic–hydrothermal ore deposits spanning about 2700 Ma of Earth history. Calculated values for $\lambda^{187}Re$ of $1.6668 \pm 0.0034 \times 10^{-11}$ year^{-1}

(using U decay constants from Jaffey *et al.* 1971) and $1.6689 \pm 0.0031 \times 10^{-11}$ $year^{-1}$ (using $\lambda^{238}U$ from Jaffey *et al.* 1971; and $\lambda^{235}U$ from Schoene *et al.* 2006) are nominally higher (0.1–0.2%) than the value determined by Smoliar *et al.* (1996), but within calculated uncertainty.

To establish the utility of the Re–Os ORS geochronometer for geological timescale calibration, Selby & Creaser (2005*a*) studied black shales from the Devonian–Mississippian (D–M) boundary of the Exshaw Formation. Black shales obtained along a narrow 10 cm stratigraphic interval straddling the D–M boundary yield a Re–Os age of 361.3 ± 2.4 Ma (Model 1, including a $\lambda^{187}Re$ uncertainty of ±0.35%, MSWD = 1.2) that agrees to within *c.* 0.2% of a recent calibration (360.7 ± 0.7 Ma) for the D–M boundary based on interpolation of U–Pb zircon dates from the lower Exshaw Formation and D–M boundary strata in New Brunswick, Canada, and Germany (Trapp *et al.* 2004). The excellent agreement between the Re–Os black shale and U–Pb zircon ages thus demonstrates the ability of the Re–Os ORS geochronometer for accurately constraining the timing, duration and rate of geological events and processes associated with sedimentary deposition.

Significance of appropriate sampling protocols for Re–Os geochronology

Another aspect of Re–Os ORS geochronology that deserves close scrutiny concerns the protocol for selecting and sampling appropriate material. This is not simply a matter of targeting ORS that have not been significantly affected by post-depositional processes such as weathering, metamorphism and hydrothermal fluid flow. For example, Selby & Creaser (2004) showed that, for a specific mineral separate, the required analysis aliquant size for obtaining reproducible and accurate Re–Os ages for molybdenite depends critically on the molybdenite grain size and age, and that small analysis aliquant sizes can result in inaccurate and/or non-reproducible Re–Os molybdenite ages. Similarly, it is necessary to determine carefully the optimal sampling strategies in order to avoid the generation of erroneous and/or imprecise Re–Os dates from ORS. The reliability of Re and Os isotope analyses can ideally be checked by replicate analyses of powder aliquots. Reproducible Re and Os abundance and isotope data for replicate analyses of a sample powder suggests a homogenous distribution of Re and Os within that powder. If Re and Os are distributed heterogeneously in a powder aliquot (incomplete powder homogenization during sample grinding), but have otherwise remained part of a closed system since deposition (negligible post-depositional mobility), then naturally coupled variations in $^{187}Re/^{188}Os$ and $^{187}Os/^{188}Os$ isotope ratios will result in reproducible sample I_{Os} with the added benefit of introducing additional variation along Re–Os isochrons (Creaser *et al.* 2002; Kendall *et al.* 2004). Significant post-depositional mobilization of Re and Os within shale samples may result in reproducible (if sample powders are homogeneous) or non-reproducible (if sample powders are heterogeneous) Re and Os abundance and isotope data for replicate analyses of powder aliquots, but in both cases the Re–Os isotope data will not yield a meaningful regression (e.g. Kendall *et al.* 2009*a*). However, it is important to distinguish between small-scale post-depositional diffusion and/or decoupling of Re and Os in otherwise pristine ORS, and large-scale element mobility resulting from some major post-depositional geological disturbance (e.g. weathering, metamorphism and hydrothermal fluid flow). Here, we demonstrate the importance of powder aliquot size for avoiding small-scale diffusion and/or elemental decoupling using ORS from the Neoproterozoic Doushantuo Formation, southern China.

The depositional age of the Doushantuo Formation is constrained by U–Pb zircon ages of 635.2 ± 0.6 and 551.1 ± 0.6 Ma from ash beds that occur near its base and top, respectively, in the Yangtze Gorges area (Fig. 2) (Condon *et al.* 2005). The latter U–Pb zircon age comes from an ash bed in the uppermost Miaohe Member (Jiuqunao section: see Zhou & Xiao 2007 for section locations) that comprises unmetamorphosed organic-rich shales with well-preserved carbonaceous compression fossils of prokaryotes, macroscopic multicellular algae and metazoans (cnidarians) (Xiao *et al.* 2002). Four samples of pyritic finely laminated black shale from the Miaohe Member (from stratigraphically lowest to highest over a *c.* 3.5 m stratigraphic interval: H_1O_{18}, H_1O_{19}, H_1O_{20}, H_1O_{21}, each comprising a volume of 40–80 cm^3) were subsampled into fractions of ≤10 g and ≥20 g of material. The samples are from the Yangtze Gorges area (Huajipo section that is less than 20 km from the Jiuqunao section: Zhou & Xiao 2007). Each subsample was ground to remove cutting marks and any weathered material, broken into small chips without metal contact and processed to a powder (*c.* 30 μm) in an automated agate mill. Rhenium and Os isotope analyses were carried out by ID-NTIMS following the methods outlined in Selby & Creaser (2001, 2003), Creaser *et al.* (2002) and Kendall *et al.* (2004), and references therein.

The Miaohe Member black shales are highly enriched in Re (30–566 ppb) and Os (1.14–8.24 ppb), and show a wide range in $^{187}Re/^{188}Os$

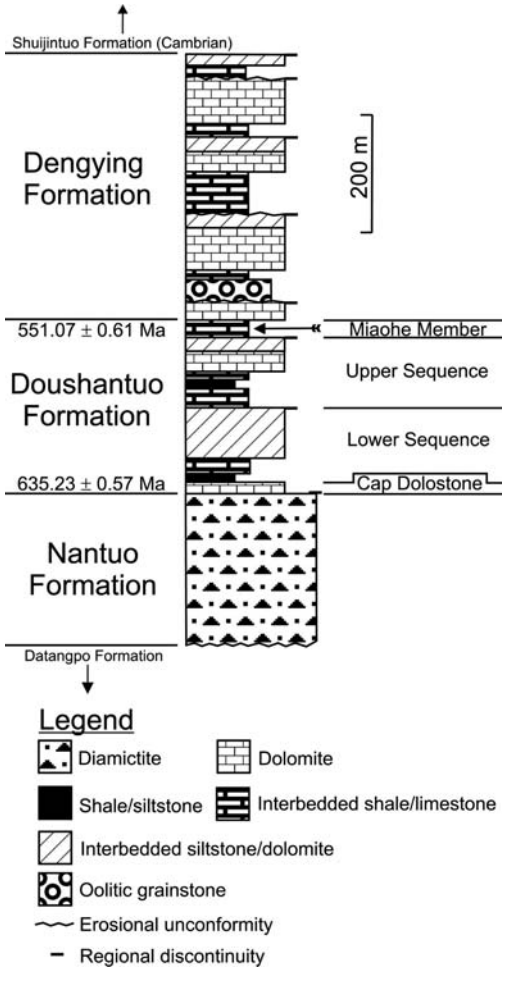

Fig. 2. Late Neoproterozoic stratigraphy, Yangtze Platform, South China. U–Pb zircon ages from ash beds are shown (Condon *et al.* 2005). The arrow indicates the sampled interval within the Miaohe Member of the uppermost Doushantuo Formation. Modified after Jiang *et al.* (2003).

(169–617) and $^{187}Os/^{188}Os$ (2.4–6.8) isotope ratios (Table 1). Duplicate analyses of ≥20 g aliquots of shale show very good reproducibility in Re and Os abundances (<3% variation), $^{187}Re/^{188}Os$ and $^{187}Os/^{188}Os$ isotope ratios (<2% variation), and $I_{Os\ (550\,Ma)}$ (≤5% variation), suggesting that Re and Os are largely distributed homogenously in these aliquots. In contrast, for ≤10 g aliquots, larger variations are observed in Re and Os abundances (up to 4% for most samples), $^{187}Re/^{188}Os$ (up to 16%) and $^{187}Os/^{188}Os$ (up to 8%) isotope ratios, and $I_{Os(550\,Ma)}$ (>20 %). These observations are independent of sample powder aliquant size used for dissolution (0.2–0.8 g). Homogeneous distribution of Re and Os in a ≥20 g aliquot suggests that a ≤10 g aliquot derived from the same whole-rock hand sample also should have a homogeneous distribution of Re and Os because grinding conditions were the same in all samples. Our samples do not show secondary alteration from weathering or hydrothermal fluid flow (e.g. quartz/carbonate veinlets were not observed), and are unmetamorphosed. Thus, the contrast in reproducibility between the two Miaohe Member subsets most probably results from small-scale post-depositional diffusion and/or decoupling of Re and Os that is preserved within the ≤10 g aliquot subset. We interpret these observations to suggest that sample powders representing a larger rock volume (≥20 g in this case) are required to remove the effect of small-scale diffusion and/or element decoupling.

Regression of all data for the Miaohe Member black shales yields a Model 3 Re–Os date of 598 ± 16 Ma (MSWD = 275; $I_{Os} = 0.65 \pm 0.13$) (Fig. 3a). Separate regressions of the ≤10 and ≥20 g aliquots yield Model 3 dates of 590 ± 20 (MSWD = 360; $I_{Os} = 0.69 \pm 0.16$) and 623 ± 13 Ma (MSWD = 16; $I_{Os} = 0.51 \pm 0.10$) (Fig. 3b, c). Although the ≥20 g aliquot sample subset yields a more precise date, all three Re–Os dates are significantly older than the U–Pb zircon age of 551.1 ± 0.6 Ma from the ash bed within the Miaohe Member. In addition, the 623 ± 13 Ma date is older than Pb/Pb phosphorite ages of 599.3 ± 4.2 (Barfod *et al.* 2002) and 576 ± 14 Ma (Chen *et al.* 2004) for the Upper Sequence of the Doushantuo Formation that stratigraphically underlies the Miaohe Member. We suggest below that this age discrepancy reflects I_{Os} heterogeneity related to temporal changes in sea-water Os isotope composition through the sampled stratigraphic interval of approximately 3.5 m.

In the Yangtze Gorges area, the Doushantuo Formation is about 250 m thick, but represents a duration of more than 80 Ma. Consequently, average sedimentation rates during Doushantuo time may have been quite slow, although at least two sequence boundaries are known to be present within the Doushantuo Formation (Xiao *et al.* 1998; Wang *et al.* 1998; Jiang *et al.* 2003; Condon *et al.* 2005; Zhou & Xiao 2007). Assuming relatively uniform sedimentation rates, the sampled stratigraphic interval of 3.5 m from the Miaohe Member could represent more than 1 Ma of elapsed time. Because of the relatively short sea-water residence time of Os (10^4 years), it is plausible that the Os isotope composition of sea water changed during the time period encompassed by the sampled stratigraphic interval. Of the ≥20 g aliquot subset, subsamples H_1O_{18}-3, H_1O_{19}-3, H_1O_{20}-4 and their replicate analyses have similar $I_{Os(550\,Ma)}$ (1.17–1.20) values and yield a Re–Os isochron

Table 1. *Re–Os abundances and isotope data for the Miaohe Member, upper Doushantuo Formation, South China*

Sample*	Aliquot mass (g)	Aliquant mass† (g)	Re (ppb)	Os (ppb)	^{192}Os (ppb)	^{187}Re/^{188}Os‡	^{187}Os/^{188}Os‡	ρ	I_{Os}§
H_1O_{18}-1	7.0	0.81	284.41	4.418	1.027	550.97 (2.30)	6.0788 (0.0110)	0.195	1.01
H_1O_{18}-1-rpt		0.80	275.38	4.510	1.049	522.45 (2.13)	6.0743 (0.0086)	0.140	1.27
H_1O_{18}-2	10.4	0.78	565.95	8.235	1.839	612.26 (2.57)	6.6343 (0.0125)	0.205	1.00
H_1O_{18}-3	39.8	0.78	402.35	6.225	1.414	566.22 (2.34)	6.3985 (0.0114)	0.166	1.19
H_1O_{18}-3-rpt		0.50	392.22	6.094	1.387	562.52 (2.32)	6.3655 (0.0120)	0.149	1.19
H_1O_{19}-1	7.8	0.80	388.52	5.971	1.388	556.92 (2.32)	6.0771 (0.0107)	0.193	0.95
H_1O_{19}-1-rpt		0.15	374.73	6.007	1.398	533.12 (2.20)	6.0583 (0.0096)	0.170	1.15
H_1O_{19}-2	6.6	0.80	392.16	5.654	1.264	617.10 (2.60)	6.6169 (0.0132)	0.212	0.94
H_1O_{19}-2-rpt		0.15	381.80	5.642	1.256	604.69 (2.88)	6.6769 (0.0258)	0.367	1.11
H_1O_{19}-2-rpt		0.79	384.57	5.715	1.265	604.89 (2.46)	6.7631 (0.0091)	0.137	1.19
H_1O_{19}-3	20.5	0.78	335.93	5.539	1.302	513.12 (2.12)	5.9227 (0.0109)	0.161	1.20
H_1O_{19}-3-rpt		0.58	338.91	5.578	1.312	513.92 (2.09)	5.9172 (0.0080)	0.129	1.19
H_1O_{20}-1	4.8	0.79	160.31	2.427	0.558	571.35 (2.42)	6.2219 (0.0127)	0.224	0.96
H_1O_{20}-1-rpt		0.26	154.73	2.490	0.579	531.48 (2.28)	6.0667 (0.0169)	0.201	1.17
H_1O_{20}-2	5.9	0.78	105.69	1.776	0.434	484.54 (2.06)	5.4170 (0.0118)	0.229	0.96
H_1O_{20}-2-rpt		0.30	102.42	1.834	0.461	441.61 (1.96)	5.0412 (0.0154)	0.272	0.98
H_1O_{20}-3	5.5	0.80	181.41	2.757	0.629	573.51 (2.41)	6.3271 (0.0128)	0.204	1.05
H_1O_{20}-3-rpt		0.25	178.81	2.809	0.647	549.62 (2.39)	6.1976 (0.0163)	0.256	1.14
H_1O_{20}-3-rpt		0.80	179.73	2.768	0.633	564.62 (2.30)	6.2948 (0.0083)	0.128	1.10
H_1O_{20}-4	22.0	0.82	167.29	2.661	0.615	541.20 (2.58)	6.1555 (0.0267)	0.331	1.17
H_1O_{20}-4-rpt		0.54	165.81	2.655	0.614	536.84 (2.20)	6.1346 (0.0086)	0.159	1.19
H_1O_{20}-5	32.8	0.78	117.44	1.945	0.464	503.58 (2.26)	5.7320 (0.0201)	0.270	1.10
H_1O_{20}-5-rpt		0.54	118.57	1.973	0.474	497.93 (2.06)	5.6414 (0.0093)	0.184	1.06
H_1O_{21}-1	8.9	0.67	33.76	1.185	0.368	182.28 (0.77)	2.6444 (0.0056)	0.180	0.97
H_1O_{21}-1-rpt		0.60	40.89	1.230	0.386	210.78 (1.01)	2.5529 (0.0103)	0.360	0.61
H_1O_{21}-1-rpt		0.75	39.09	1.206	0.377	206.27 (0.86)	2.5846 (0.0048)	0.192	0.69
H_1O_{21}-2	4.6	0.53	32.88	1.139	0.358	182.60 (0.78)	2.5224 (0.0051)	0.210	0.84
H_1O_{21}-2-rpt		0.62	34.52	1.175	0.373	184.00 (0.81)	2.4290 (0.0071)	0.246	0.74
H_1O_{21}-2-rpt		0.74	30.44	1.140	0.359	168.59 (0.70)	2.5037 (0.0043)	0.187	0.95
H_1O_{21}-3	32.2	0.49	37.09	1.176	0.368	200.68 (0.87)	2.5825 (0.0065)	0.279	0.74
H_1O_{21}-3-rpt		0.46	36.59	1.181	0.369	197.08 (0.89)	2.5864 (0.0082)	0.312	0.77

*rpt denotes a replicate analysis.
†Used for individual Re–Os analysis.
‡Numbers in parentheses denote measured 2σ uncertainty in the isotope ratio calculated by numerical error propagation.
§I_{Os}, initial ^{187}Os/^{188}Os isotope ratio calculated at 550 Ma.

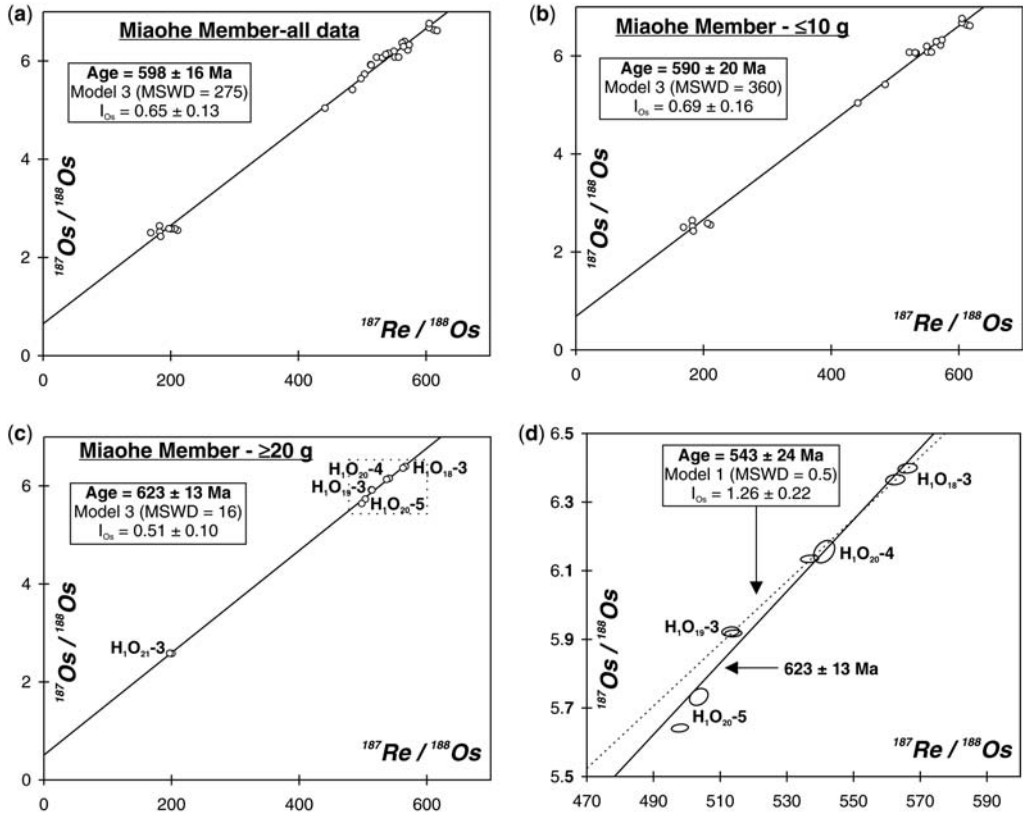

Fig. 3. Re–Os isochron diagrams for the Neoproterozoic Miaohe Member, uppermost Doushantuo Formation, South China. (**a**) All data. (**b**) Subset from ≤10 g sample aliquots. (**c**) Subset from ≥20 g aliquots. (**d**) Expanded view of the inset diagram in (c). Three samples (H_1O_{18}-3, H_1O_{19}-3 and H_1O_{20}-4) have similar $I_{Os\ (550\,Ma)}$ of 1.17–1.20 and plot on a 543 ±24 Ma Model 1 isochron, but samples H_1O_{20}-5 and H_1O_{21}–3 (not shown) have less radiogenic $I_{Os\ (550\,Ma)}$ of 1.06–1.10 and 0.74–0.77, respectively, and plot below this isochron. Because sample H_1O_{21}-3 has much lower $^{187}Re/^{188}Os$ and $^{187}Os/^{188}Os$ relative to the other samples, it effectively controls the slope of an isochron defining an erroneously old Re–Os date of 623 ± 13 Ma. Regressions used measured 2σ uncertainties for $^{187}Re/^{188}Os$ and $^{187}Os/^{188}Os$, and the error correlation function (ρ) (Ludwig 1980; Kendall *et al.* 2004).

age of 543 ± 24 Ma (Model 1, MSWD = 0.5; I_{Os} = 1.26 ± 0.22) that is imprecise because of the restricted range in Re/Os, but overlaps the U–Pb zircon age of 551.1 ± 0.6 Ma for the Miaohe Member (Fig. 3d). However, both analyses of sample H_1O_{20}-5 do not plot on this regression, and have less radiogenic $I_{Os\ (550\,Ma)}$ values of 1.06–1.10 suggesting a possible change in sea water Os isotope composition is recorded within whole-rock H_1O_{20} (volume 80 cm^3). The stratigraphically highest subsample H_1O_{21}-3 has the lowest $I_{Os\ (550\,Ma)}$ values (0.74–0.77) and is characterized by a significantly less radiogenic Os isotope composition compared to the other ≥20 g aliquots. Thus, this one subsample exerted a large effect on the ≥20 g aliquot regression, which resulted in an erroneously old age estimate of 623 ± 13 Ma. The Miaohe Member Re–Os data demonstrate that a deceptively attractive date can be obtained for a sample suite with heterogeneous I_{Os}, especially when there is a large, but skewed, distribution in $^{187}Re/^{188}Os$ and $^{187}Os/^{188}Os$ isotope ratios.

Because of the potentially slow sedimentation rates for some condensed black shale sequences (e.g. <2 m Ma^{-1}: Arthur & Sageman 1994), a relatively short sea-water residence time for Os (probably $<10^4$ years in low-O_2 Proterozoic oceans) and potential for rapid variations in sea-water $^{187}Os/^{188}Os$, a thin stratigraphic sampling interval is critical to obtain homogenous I_{Os}. A thin stratigraphic sampling interval, together with a sufficiently large mass of black shale powder (e.g. >20 g), are thus key sampling protocols for precise and accurate Re–Os depositional age

determinations. Recent studies have successfully produced precise Model 1 Re–Os ages for shales from stratigraphic intervals ranging from tens of centimetres to a few metres, and by using powder aliquots comprising >20 g of powdered shale (Kendall *et al.* 2004, 2006, 2009*a*, *b*; Selby & Creaser 2005*a*; Anbar *et al.* 2007; Creaser & Stasiuk 2007).

Discrepancy in Re–Os dates for the Neoproterozoic Aralka Formation, central Australia

Using the inverse aqua regia dissolution protocol, Schaefer & Burgess (2003) reported Re–Os dates of 592 ± 14 ($n = 3$, MSWD ≪1; $I_{Os} = 0.91 \pm 0.07$) and 623 ± 18 Ma ($n = 7$, MSWD = 5.2; $I_{Os} = 0.78 \pm 0.10$) for organic-rich dolomitic siltstones (TOC *c.* 0.5–1%) of the Aralka Formation (Amadeus Basin, central Australia). Because the seven samples defining the 623 ± 18 Ma date spanned a stratigraphic interval of about 10 m that could potentially be characterized by heterogeneous I_{Os}, Schaefer & Burgess (2003) suggested that the regression defined by the three samples in closest stratigraphic proximity (*c.* 1.6 m) represented the best estimate of the true depositional age. However, Kendall *et al.* (2006) subsequently obtained a significantly older Re–Os date of 657.2 ± 5.4 Ma (MSWD = 1.2; $I_{Os} = 0.82 \pm 0.03$) by Cr^{VI}–H_2SO_4 digestion of 18 samples (and two replicates) derived from *c.* 2 m stratigraphic interval within the larger 10 m interval sampled by Schaefer & Burgess (2003) (Fig. 4).

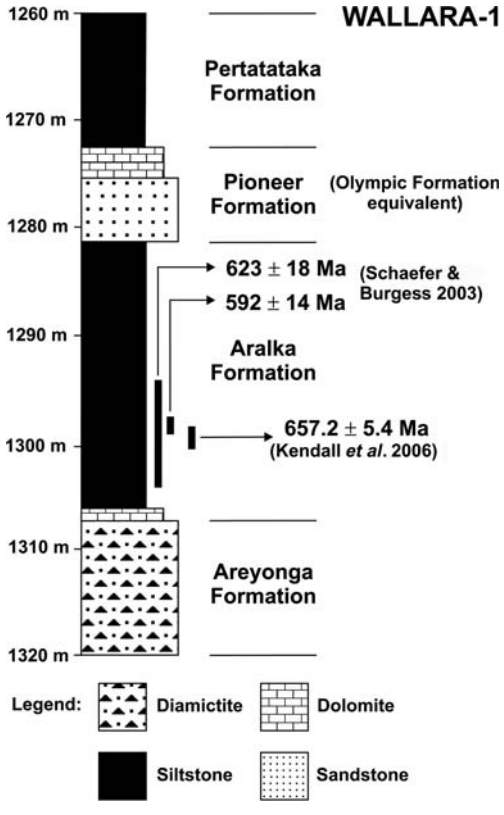

Fig. 4. Stratigraphic column for drillhole Wallara-1 (Amadeus Basin, central Australia) showing sampled intervals and Re–Os dates obtained for organic-rich siltstones of the Neoproterozoic Aralka Formation by Schaefer & Burgess (2003) and Kendall *et al.* (2006). Modified from Schaefer & Burgess (2003).

To determine whether the reason for this age discrepancy was simply the nature of the digestion mediums used (as suggested by Kendall *et al.* 2004), we reanalysed three of our Aralka Formation samples (BK-04-Wallara-1A, BK-04-Wallara-2A and BK-04-Wallara-5) using inverse aqua regia (Table 2). Our initial analyses used approximately 1.44–1.48 g of shale powder for Carius Tube digestion, and plot near the *c.* 623 Ma-isochron of Schaefer & Burgess (2003) (Fig. 5). However, replicate analyses for BK-04-Wallara-1A and BK-04-Wallara-5 using the same amount of sample powder were not reproducible in terms of Re and Os abundances, $^{187}Re/^{188}Os$ and $^{187}Os/^{188}Os$ isotope ratios, and $I_{Os\ (657\,Ma)}$. The large degree of scatter indicated to us that sample-spike equilibration had not occurred for these replicate analyses during Carius tube digestion. Subsequently, replicate analyses used 0.50–0.54 g of powder for inverse aqua regia digestion, and these data plot near the *c.* 657 Ma-isochron defined by the Cr^{VI}–H_2SO_4 analyses of Kendall *et al.* (2006). In addition, the *c.* 0.50–0.54 g inverse aqua regia analyses have broadly similar Re and Os abundances, $^{187}Re/^{188}Os$ and $^{187}Os/^{188}Os$ isotope ratios, and $I_{Os\ (657\,Ma)}$ as the Cr^{VI}–H_2SO_4 analyses from the same powder aliquots. Regression of our 0.50–0.54 g inverse aqua regia subset yields a Model 1 Re–Os date of 657 ± 15 Ma (MSWD = 0.7; $I_{Os} = 0.87 \pm 0.09$) that is statistically equivalent to the *c.* 657 Ma age obtained using Cr^{VI}–H_2SO_4 digestion. To obtain a direct estimate of the Re–Os systematics of the detrital component, we carried out an inverse aqua regia attack on the Carius tube residue left behind after Cr^{VI}–H_2SO_4 digestion of sample BK-04-Wallara-5. The Re–Os data for this residue have large uncertainty, but plot on the isochrons of both Schaefer & Burgess (2003) and Kendall *et al.* (2006) near the I_{Os} intercept. However, the residue has a calculated $I_{Os\ (657\,Ma)}$ of 0.85 similar to calculated $I_{Os\ (657\,Ma)}$ values of

Table 2. *Re–Os isotope data derived from inverse aqua regia and Cr^{VI}–H_2SO_4 digestions of three Aralka Formation samples*

Sample	Method*	Aliquant mass[†] (g)	Re (ppb)	Os (ppt)	^{192}Os (ppt)	$^{187}Re/^{188}Os$[‡]	$^{187}Os/^{188}Os$[‡]	ρ	I_{Os}[§]
BK-04-Wallara-1A	Cr^{VI}–H_2SO_4[a]	1.06	5.41	145.9	41.0	262.10 (1.23)	3.7170 (0.0125)	0.525	0.83
	Cr^{VI}–H_2SO_4-rpt[a]	1.48	5.41	145.3	40.9	263.41 (1.20)	3.7149 (0.0129)	0.436	0.82
	IAR[b]	1.45	6.01	145.0	40.8	293.02 (1.30)	3.7190 (0.0127)	0.331	0.49
	IAR-rpt[b]	1.46	5.36	148.1	41.8	255.03 (1.38)	3.6755 (0.0166)	0.642	0.87
	IAR-rpt[b]	0.54	5.33	146.7	41.4	256.18 (3.68)	3.6721 (0.0660)	0.747	0.85
BK-04-Wallara-2A	Cr^{VI}–H_2SO_4[a]	1.02	5.18	125.3	33.9	304.28 (1.54)	4.1659 (0.0164)	0.596	0.82
	IAR[b]	1.46	5.12	176.1	54.7	186.27 (0.91)	2.6518 (0.0097)	0.561	0.60
	IAR-rpt[b]	0.50	4.88	122.5	33.4	291.15 (4.14)	4.0802 (0.0611)	0.885	0.88
BK-04-Wallara-5	Cr^{VI}–H_2SO_4[a]	0.99	4.38	81.8	19.5	447.17 (3.28)	5.7469 (0.0421)	0.746	0.83
	Cr^{VI}–H_2SO_4-rpt[a]	1.49	4.36	81.8	19.5	443.99 (2.71)	5.7200 (0.0354)	0.625	0.83
	IAR[b]	1.48	4.67	87.5	22.0	421.86 (2.14)	5.0383 (0.0254)	0.421	0.40
	IAR-rpt[b]	1.44	4.34	85.5	19.7	437.89 (3.77)	6.2048 (0.0517)	0.843	1.39
	IAR-rpt[b]	0.52	4.44	84.3	20.2	438.58 (9.32)	5.7034 (0.1241)	0.946	0.88
	IAR-rpt[b]	0.51	4.18	79.8	19.2	434.01 (4.48)	5.6272 (0.0742)	0.677	0.85
	Cr^{VI}–H_2SO_4-res[b]	0.87	0.01	2.3	0.8	27.26 (6.45)	1.1466 (0.1803)	0.432	0.85

*rpt, IAR and res denote replicate, inverse aqua regia and residue analysis by IAR, respectively; [a]data from Kendall *et al.* (2006); [b]data from this study.
[†]Used for individual Re–Os analysis.
[‡]Numbers in parentheses denote measured 2σ uncertainty in the isotope ratio calculated by numerical error propagation.
[§]$I_{Os} = {}^{187}Os/{}^{188}Os$ isotope ratio calculated at 657 Ma (from Kendall *et al.* 2006).

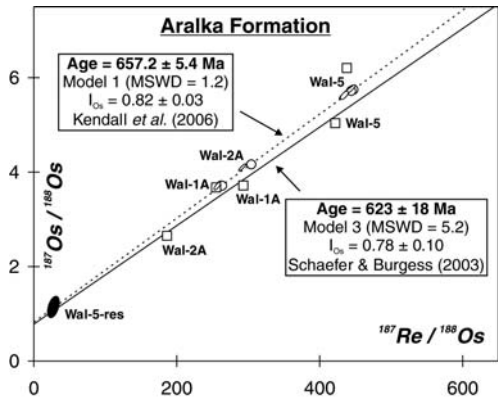

Fig. 5. Re–Os isochron diagram for the Aralka Formation showing the inverse aqua regia and Cr^{VI}–H_2SO_4 linear regressions from Schaefer & Burgess (2003) and Kendall *et al.* (2006), respectively. For clarity, only individual sample analyses of BK-04-Wallara-1A, BK-04-Wallara-2A and BK-04-Wallara-5 are shown. Circles, Cr^{VI}–H_2SO_4 analyses (Kendall *et al.* 2006); error ellipses, inverse aqua regia analyses using an aliquant size of *c.* 0.5 g (this study); squares, inverse aqua regia analyses using an aliquant size of *c.* 1.4–1.5 g (this study). Regression of the *c.* 0.5 g inverse aqua regia subset yields a Model 1 Re–Os date (not shown) of 657 ± 15 Ma (MSWD = 0.7; I_{Os} = 0.87 ± 0.09) that is equivalent within 2σ uncertainties to the Cr^{VI}–H_2SO_4 isochron age reported by Kendall *et al.* (2006). The inverse aqua regia analysis of the residue from Cr^{VI}–H_2SO_4 digestion of sample BK-04-Wallara-5 (Wal-5-res) provides an estimate of the detrital Re–Os systematics in the Aralka Formation and is shown for comparison.

0.81–0.84 for Cr^{VI}–H_2SO_4 analyses (Kendall *et al.* 2006), but is more radiogenic than calculated $I_{Os\ (657\ Ma)}$ values of 0.47–0.71 from the data of Schaefer & Burgess (2003). The similar ages derived here using the two dissolution mediums, together with the Re–Os data for the residue, suggests the detrital component in the Aralka Formation is minor and/or has similar I_{Os} as the hydrogenous Os fraction. Accordingly, the discrepancy between the Re–Os data of Schaefer & Burgess (2003) and Kendall *et al.* (2006) may relate to incomplete sample-spike equilibration during inverse aqua regia digestion of large (e.g. 1.4–1.5 g) aliquant fractions. In contrast, reproducible Re–Os data diagnostic of complete sample-spike equilibration during Cr^{VI}–H_2SO_4 digestions was obtained for the Aralka Formation using up to 1.5 g of sample (Kendall *et al.* 2006). Because sample details were not provided by Schaefer & Burgess (2003), further comparison with the data reported here and in Kendall *et al.* (2006) is not possible.

The $^{187}Os/^{188}Os$ isotope composition of Precambrian sea water

The value of I_{Os} from a Re–Os ORS isochron regression may record the $^{187}Os/^{188}Os$ isotope composition of the contemporaneous sea water at the time of sediment deposition if the hydrogenous Os fraction dominates the detrital/extraterrestrial Os fraction of ORS (Ravizza & Turekian 1989, 1992; Ravizza *et al.* 1991). This tenet is supported by the similar Os isotope composition of recent organic-rich sediments ($^{187}Os/^{188}Os$ = 0.98–1.07 based on data from three localities in the Pacific and Atlantic oceans) compared to present-day sea water (Ravizza & Turekian 1992). Similarly, Ravizza & Paquay (2008) show that Eocene–Oligocene organic-rich sediments yield initial Os isotope ratios (calculated using depositional ages derived from biostratigraphy) that agree well with Os isotope data from pelagic carbonates (which do not require correction for *in situ* decay of ^{187}Re to ^{187}Os). Because the present-day sea-water residence time of Os (10^4 years) is long compared to the ocean mixing time (2–3 ka), large global variations in the $^{187}Os/^{188}Os$ isotope composition of sea water are suggested to have occurred during the Cenozoic and Mesozoic. These variations result from major changes in the proportion of radiogenic Os (from oxidative weathering of upper continental crust) and unradiogenic Os (from dissolution of cosmic dust and hydrothermal alteration of oceanic crust and peridotites) delivered to the oceans (Peucker-Ehrenbrink *et al.* 1995; Pegram & Turekian 1999; Ravizza *et al.* 2001; Cohen & Coe 2002, 2007; Ravizza & Peucker-Ehrenbrink 2003; Cohen 2004; Cohen *et al.* 2004).

Determination of the Os isotope composition of Precambrian sea water is limited to a handful of I_{Os} determinations from precise Re–Os isochron regressions of Proterozoic and latest Archaean ORS (Hannah *et al.* 2004, 2006; Kendall *et al.* 2004, 2006, 2009*a*, *b*; Anbar *et al.* 2007; Creaser & Stasiuk 2007; Yang *et al.* 2009). The sea-water residence time of Os was probably low under conditions of a predominantly anoxic Archaean atmosphere and ocean prior to the 2.45–2.32 Ga Great Oxidation Event (Farquhar *et al.* 2000; Pavlov & Kasting 2002; Bekker *et al.* 2004; Goldblatt *et al.* 2006), or in a stratified Proterozoic ocean with oxidizing surface waters and suboxic, anoxic or euxinic deep waters after the Great Oxidation Event (Canfield 1998; Farquhar & Wing 2003; Slack *et al.* 2007). The deep ocean may not have become fully oxygenated until the Neoproterozoic (e.g. Fike *et al.* 2006; Kennedy *et al.* 2006; Canfield *et al.* 2007). On the modern Earth a restricted or semi-restricted (e.g. intracratonic) depositional environment can lead to preservation of I_{Os} in

ORS that reflects local sea water, but not the contemporaneous global sea water (Ravizza *et al.* 1991; Martin *et al.* 2000; Poirer 2006). Thus, a significantly shorter residence time of Os in Precambrian sea water would likely be accompanied by regional variations in sea-water Os isotope composition.

Nevertheless, some interesting insights can be gained from the limited information available for the Os isotope composition of Precambrian seawater. Weathering of ORS represents a major source of radiogenic Os to the Phanerozoic oceans (Peucker-Ehrenbrink & Hannigan 2000; Peucker-Ehrenbrink & Ravizza 2000; Jaffe *et al.* 2002; Pierson-Wickmann *et al.* 2002). However, for a predominantly anoxic Archaean atmosphere and oceans, riverine transport of soluble Re and radiogenic Os from weathering and erosion of crustal rocks would be negligible, resulting in deposition of Archaean shales with low Re abundances and $^{187}Re/^{188}Os$ and $^{187}Os/^{188}Os$ ratios (Yang & Holland 2002; Siebert *et al.* 2005; Wille *et al.* 2007). There may also have been a time lag between the Great Oxidation Event and appreciable riverine transport of radiogenic crustal Os to the oceans because of the low Re abundances in uplifted Archaean shales and/or insufficiently oxidizing conditions (Hannah *et al.* 2004). Chondritic or near-chondritic I_{Os} compositions may be typical of marine shales deposited under an anoxic weathering regime or under the conditions of a weakly oxygenated [e.g. 10^{-5}–10^{-2} PAL (present atmospheric level) for *c.* 2.45–2.00 Ga (Ga is 10^9 years): Farquhar & Wing 2003] or anoxic atmosphere with stratified oceans containing oxygenated shallow waters and anoxic or euxinic deep waters (Hannah *et al.* 2004, 2006; Siebert *et al.* 2005; Anbar *et al.* 2007; Wille *et al.* 2007). Chondritic I_{Os} values (e.g. *c.* 0.11) obtained from the 2.7 Ga Joy Lake Sequence, Superior Province, USA (Yang *et al.* 2009), the 2.50 Ga Mt McRae Shale, Hamersley Group, western Australia (Anbar *et al.* 2007) and 2.32 Ga Rooihoogte and Timeball Hill Formations, Transvaal Supergroup, South Africa (Hannah *et al.* 2004) are consistent with dominance of the late Archaean–early Palaeoproterozoic marine Os budget by extraterrestrial and magmatic/hydrothermal inputs (Fig. 6). If Earth's atmosphere and oceans were fully anoxic for most of the Archaean, depositional age determinations for most Archaean shales would not be feasible. In this case, the fundamental basis behind the Re–Os ORS geochronometer, namely the reductive capture of dissolved Re from an oxygenated water column into reducing ORS, breaks down. Such shales would be characterized by a subequal mixture comprising meteoritic and hydrogenous components with low Re/Os and chondritic $^{187}Os/^{188}Os$, and a detrital component with relatively higher Re/Os (radiogenic sulphides would persist as detrital phases during anoxic weathering and erosion: e.g. Fleet 1998; Rasmussen & Buick 1999; England *et al.* 2002) and elevated $^{187}Os/^{188}Os$.

Of particular interest is a precise determination of the time when pO_2 in the atmosphere rose sufficiently to allow oxidative weathering of continental crust and the development of a significant riverine flux of radiogenic Os to the oceans. The limited information available for the Os isotope composition of Precambrian sea water does not yet provide this information. A chondritic I_{Os} value of 0.133 ± 0.020 for *c.* 2.0 Ga sea water ('Productive Formation', Pechenga Greenstone Belt, Russia) may reflect a minimal riverine flux of radiogenic Os and/or dominance of mantle inputs in a rift-related tectonic setting (Hannah *et al.* 2006). A large time gap in the curve for Precambrian sea-water Os isotope compositions (see Fig. 6) exists until 1.54 Ga, where a I_{Os} determination of 0.51 ± 0.03 for the Douglas Formation (Athabasca Basin, western Canada) clearly indicates that crustal weathering and transport of radiogenic Os to sea water was possible during the Mesoproterozoic (Creaser & Stasiuk 2007). Two Re–Os isochron ages from the *c.* 1.4 Ga Velkerri Formation (McArthur Basin, northern Australia) yield I_{Os} values of 0.29 ± 0.18 and 0.06 ± 0.22 (Kendall *et al.* 2009*a*) that also permit some contribution of dissolved radiogenic crustal Os to *c.* 1.4 Ga oceans. By Late Neoproterozoic time, however, crustal Os fluxes from rivers exerted a significant control on the $^{187}Os/^{188}Os$ isotope composition of sea water. This is evidenced by moderate or radiogenic I_{Os} from the *c.* 657 Ma Aralka Formation, central Australia (0.82 ± 0.03), *c.* 643 Ma Tindelpina Shale Member, Tapley Hill Formation, southern Australia (0.95 ± 0.01), *c.* 640 Ma Black River Dolomite, northwestern Tasmania (1.00 ± 0.05), *c.* 608 Ma Old Fort Point Formation, western Canada (0.62 ± 0.03) and *c.* 551 Ma Miaohe Member, Doushantuo Formation (1.26 ± 0.22) (Kendall *et al.* 2004, 2006, 2009*b*; this study). Delineation of the broad features of the Proterozoic sea-water $^{187}Os/^{188}Os$ curve will depend upon further determination of I_{Os} values from precise Re–Os age determinations of ORS.

Re–Os geochronology of Precambrian ORS

With rigorous sampling and analytical protocols, the ^{187}Re–^{187}Os system can yield precise and accurate depositional ages for Precambrian ORS. In many Precambrian sedimentary basins (e.g.

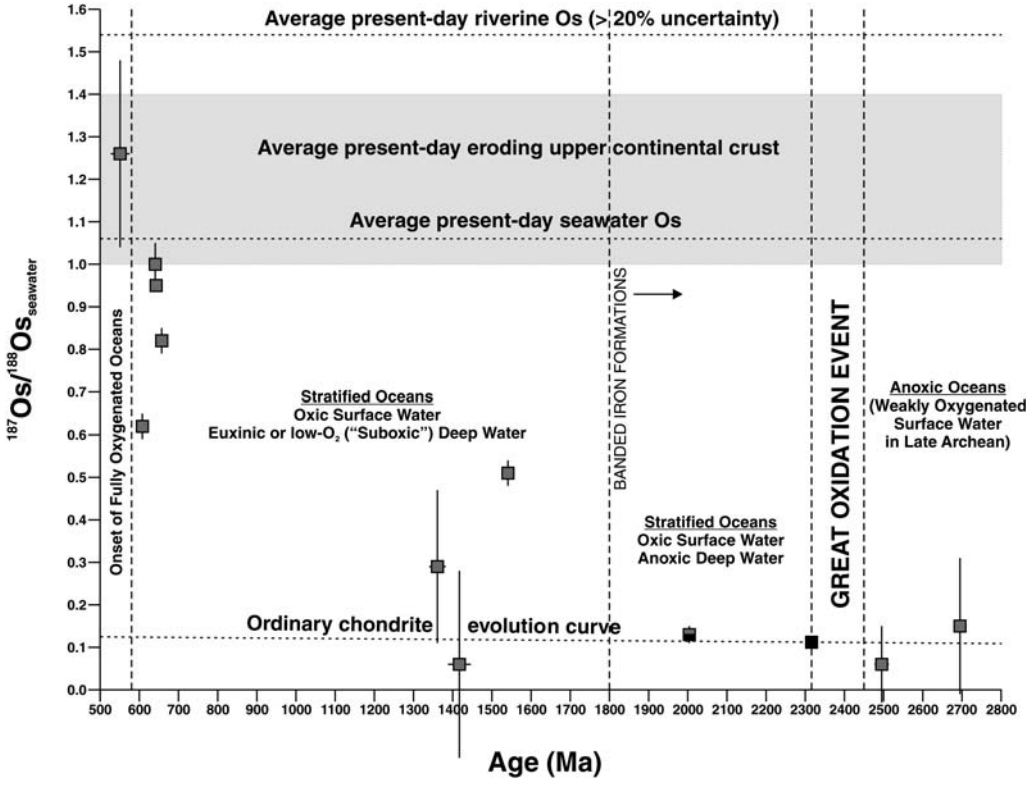

Fig. 6. Precambrian sea-water Os isotope compositions derived from black shale Re–Os isochron regressions of ORS. The suggested timeline for Precambrian Earth surface oxygenation is also shown for comparison. See text for discussion and sources of data. Grey squares, isochron regression I_{Os} derived from Cr^{VI}–H_2SO_4 digestion of ORS; black square, isochron regression I_{Os} derived from synsedimentary–early diagenetic pyrite in ORS; grey and black square, isochron regression I_{Os} derived using both methods. The 2.5 Ga Mt McRae Shale Re–Os age gave a subchondritic I_{Os} of 0.04 ± 0.06, but this age was derived from two sample subsets that were separated by more than 15 m of stratigraphy (Anbar *et al.* 2007). Because it is possible that the two sampled stratigraphic intervals may record distinctive sea-water Os isotope compositions, only the I_{Os} derived from Re–Os isochron regressions of the individual subsets ($I_{Os} = 0.86 \pm 0.86$ and 0.06 ± 0.09) may represent a robust estimate of the sea-water Os isotope composition. The more precise determination ($I_{Os} = 0.06 \pm 0.09$) is shown in the figure.

Neoproterozoic Windermere Supergroup, Mackenzie Mountains, Canada: Narbonne & Aitken 1995), ORS are typically more common than volcanic tuff horizons suitable for U–Pb zircon dating, so Re–Os ages from ORS may hold great promise for radiometric calibration of the Precambrian geological timescale. Nearly all precise Re–Os ages obtained from Precambrian ORS (described later) have been obtained using drill core, which avoids the issue of post-depositional mobility of Re and Os from ORS during oxidative surface weathering (Peucker-Ehrenbrink & Hannigan 2000; Jaffe *et al.* 2002; Pierson-Wickmann *et al.* 2002). Development of programmes for the acquisition of drill cores from Precambrian sedimentary successions (e.g. the Astrobiology Drilling Program of the NASA Astrobiology Institute) and preservation of drill core from petroleum exploration wells are thus important for successful Re–Os ORS geochronological studies and an improved Precambrian chronostratigraphy. Furthermore, organic-rich shales of Proterozoic age are increasingly being targeted as hydrocarbon source rocks for petroleum exploration. Several major oil-producing fields are known (e.g. Huqf Supergroup of Oman, Centralian Superbasin of Australia and the Siberian Craton: Peters *et al.* 2005) and exploration in Proterozoic basins is underway on most continents (e.g. Lottaroli & Craig 2006). Here, we review recent applications of the Re–Os system to Precambrian ORS that have constrained the timing of Proterozoic glaciations, Earth surface oxygenation and the depositional age of organic-rich shales with potential for generating hydrocarbons.

Timing of Neoproterozoic glaciation

Fine-grained siliciclastic sedimentary rocks such as siltstones and shales are commonly deposited during the post-glacial, eustatic sea-level rise that accompanies the end of major episodes of glaciation. If such mudrocks are organic-rich and were deposited under oxygen deficient, anoxic or suboxic conditions, they represent attractive targets for Re–Os geochronology because a Re–Os age would provide a minimum age constraint on the end of glaciation. This approach was one solution proposed to counter the large degree of uncertainty surrounding the number, timing, extent and duration of Neoproterozoic glaciations. These uncertainties result from a scarcity of suitable acid igneous rocks for U–Pb zircon dating of most Neoproterozoic glacial deposits (Schaefer & Burgess 2003; Kendall *et al.* 2004, 2006).

Kendall *et al.* (2004) obtained a Model 1 Re–Os age of 607.8 $\pm$ 4.7 Ma (see Fig. 1) for the Old Fort Point Formation (OFP), a widespread post-glacial marker horizon interpreted as the deep-water facies equivalent of cap carbonates overlying glacial deposits in the middle Windermere Supergroup (Ross *et al.* 1995). The significance of the Re–Os age for dating post-glacial sedimentation relied on lithostratigraphic correlations between the dated OFP interval from the Rocky Mountains, western Alberta (where no glacial deposits are preserved) and stratigraphic successions in northeastern British Columbia and the Mackenzie Mountains, N.W.T., that contain the glaciogenic Vreeland and Ice Brook formations (and their cap carbonates), respectively (Ross *et al.* 1995). Based on the geochronological database available for Neoproterozoic glaciation, Kendall *et al.* (2004) suggested that the Vreeland–Ice Brook glaciation represents part of a *c.* 620–600 Ma glaciation (e.g. represented, in part, by the Nantuo Formation, southern China: Barfod *et al.* 2002). Subsequently, new precise U–Pb zircon age constraints have been obtained for the Doushantuo Formation cap carbonate overlying the Nantuo Formation (635.23 $\pm$ 0.57 Ma: Condon *et al.* 2005) and the Ghaub Formation, Namibia (635.51 $\pm$ 0.54 Ma: Hoffmann *et al.* 2004). In light of these new age constraints, it is possible that the Vreeland–Ice Brook glaciation may have been wholly or partly younger than *c.* 635 Ma. Alternatively, if the Vreeland–Ice Brook glaciogenic diamictites represent part of a global glaciation that ended at *c.* 635 Ma (Condon *et al.* 2005), then the Re–Os age of 607.8 $\pm$ 4.7 Ma for the OFP may simply reflect a relatively condensed section (*c.* 80–120 m thick: Ross *et al.* 1995) and the underlying coarse-grained sandstones that are laterally equivalent to the Vreeland diamictites (Hein & McMechan 1994; McMechan 2000).

Prior to the study by Kendall *et al.* (2006), direct age constraints for the Sturtian and Elatina Formation glacial deposits of southern Australia were particularly poor, with the best age constraint being a U–Pb zircon age of 777 $\pm$ 7 Ma from volcanic rocks more than 6 km below Sturtian glacial deposits (Preiss 2000). Nevertheless, the Sturtian and Elatina Formation glacial deposits have served as marker horizons for global correlation schemes based largely on litho- and chemo-stratigraphy (Kennedy *et al.* 1998; Walter *et al.* 2000; Halverson *et al.* 2005). Kendall *et al.* (2006) tested proposed correlation schemes for a putative global 'Sturtian' ice age by obtaining Re–Os ages from post-glacial black shales immediately overlying Sturtian and Areyonga glaciogenic diamictites in drill cores from southern and central Australia, respectively. Two Re–Os ages of 647 $\pm$ 10 (Model 1, MSWD = 0.79) and 645.1 $\pm$ 4.8 Ma (Model 1, MSWD = 1.2) were obtained for the Tindelpina Shale Member (basal Tapley Hill Formation, Adelaide Rift Complex, southern Australia) from two separate drill cores (Fig. 7a). The sampled intervals from the two cores can be correlated on the basis of carbon isotope chemostratigraphy. Thus, combining the Re–Os data from both drill cores resulted in a depositional age of 643.0 $\pm$ 2.4 Ma (Model 1, MSWD = 1.1) for the Tindelpina Shale Member. A Re–Os age of 657.2 $\pm$ 5.4 Ma (Model 1, MSWD = 1.2) was also obtained for the Aralka Formation (Amadeus Basin, central Australia) from a single drill core. Because both diamictite–shale contacts appear conformable, the Re–Os ages were interpreted as tight minimum age constraints for the end of Sturtian and Areyonga glaciation. The new Re–Os ages suggested that the Sturtian and Areyonga glacial intervals were significantly younger than other radiometrically dated (*c.* 685–750 Ma) glacial intervals previously regarded as possible correlatives. A U–Pb SHRIMP zircon age of 659 $\pm$ 6 Ma from a tuffaceous bed within the glaciogenic Sturtian Wilyerpa Formation (Fanning & Link 2008) supports the interpretations of Kendall *et al.* (2006). Thus, the Sturtian ice age was diachronous and/or there were multiple episodes of 'Sturtian' glaciation between about 750 and 643 Ma, each of uncertain duration and extent.

Late Mesoproterozoic glaciation in Brazil?

The Vazante Group of the Sao Francisco Basin (east-central Brazil) represents another Precambrian sedimentary succession with glaciogenic

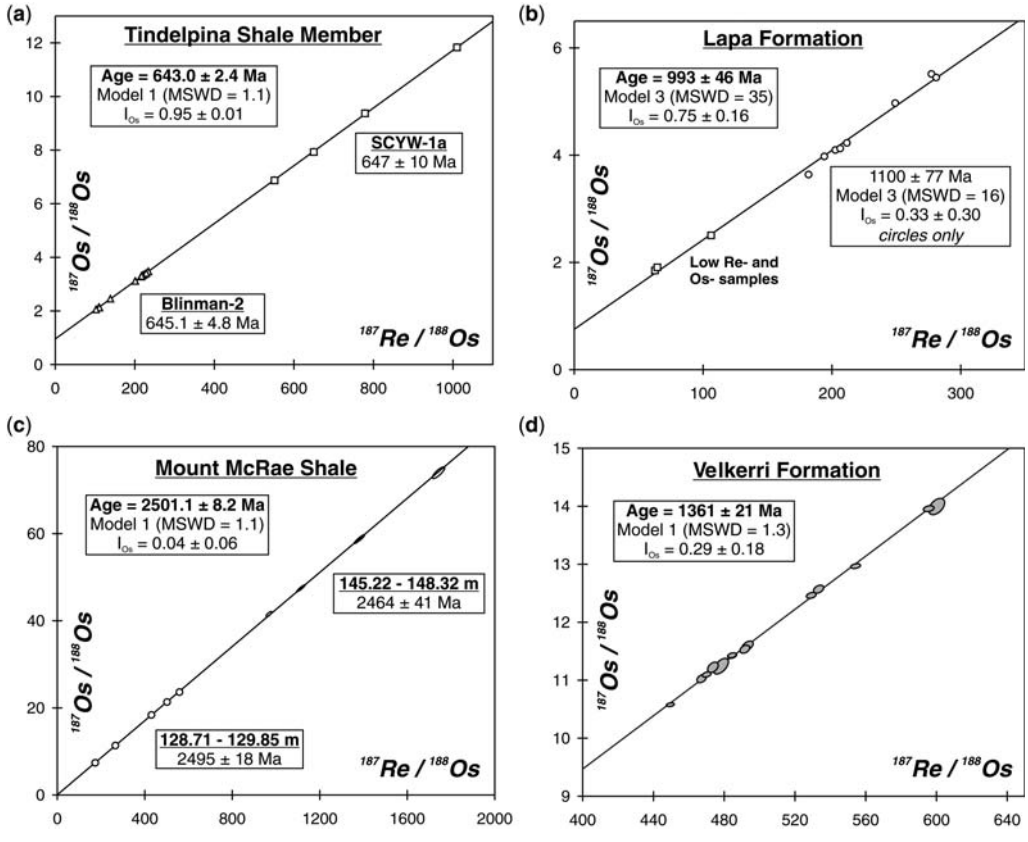

Fig. 7. Examples of Re–Os isochrons for Precambrian ORS. (**a**) Neoproterozoic Tindelpina Shale Member, basal Tapley Hill Formation, Adelaide Rift Complex, South Australia (Kendall *et al.* 2006). Triangles, Blinman-2 drillhole; squares, SCYW-1a drillhole. (**b**) Late Mesoproterozoic Lapa Formation, upper Vazante Group, Brasilia Fold Belt, Brazil (Azmy *et al.* 2008). Exclusion of the three low Re- and Os-samples (squares) yields a nominally older date of 1100 ± 77 Ma (Model 3, MSWD = 16; I_{Os} = 0.33 ± 0.30; circles). (**c**) Late Archaean M McRae Shale, Hamersley Basin, western Australia (Anbar *et al.* 2007). Depth intervals refer to two stratigraphic horizons (represented by error ellipses and circles) sampled from the ABDP-9 drillhole. (**d**) Mesoproterozoic Velkerri Formation (upper organic-rich interval), McArthur Basin, northern Australia (Kendall *et al*. 2009*a*). All regressions used measured 2σ uncertainties for $^{187}Re/^{188}Os$ and $^{187}Os/^{188}Os$, and the error correlation function (ρ).

diamictites and cap carbonates, and is characterized by a paucity of reliable U–Pb radiometric age constraints. Distinctive negative $\delta^{13}C$ isotope excursions in the cap carbonate, together with $^{87}Sr/^{86}Sr$ data (Azmy *et al.* 2001, 2006; Brody *et al.* 2004; Olcott *et al.* 2005), were used to correlate the upper Vazante Group diamictite unit and overlying post-glacial cap carbonate (Lapa Formation) with the $<746 \pm 2$ Ma (Hoffman *et al.* 1996) glaciogenic Chuos Formation and Rasthof Formation cap carbonate on the Congo Craton, Namibia (Azmy *et al.* 2001, 2006). However, a Re–Os date of 993 ± 46 Ma (Model 3, MSWD = 35; I_{Os} = 0.75 ± 0.16) was obtained for ORS at the base of the Lapa Formation (Fig. 7b) (Azmy *et al.* 2008). Exclusion of three samples with low Re (0.4–0.9 ppb) and Os (33–54 ppt) abundances (e.g. possible significant detrital component) yields a nominally older Re–Os date of 1100 ± 77 Ma (Model 3, MSWD = 16; I_{Os} = 0.33 ± 0.30). Elevated MSWD in these regressions may reflect post-depositional mobilization (e.g. chlorite-grade metamorphism or hydrothermal fluid flow), and/or heterogeneous sea-water I_{Os} (samples were derived from a *c.* 15 m stratigraphic interval to obtain a good range of Re/Os ratios). However, the Re–Os dates were suggested to represent a good estimate of the depositional age for the basal Lapa Formation on the basis of reasonable I_{Os} derived from the Re–Os isochron regressions, the absence of upper Vazante Group and basal Lapa Formation detrital zircons yielding concordant U–Pb ages

younger than about 1000 Ma, and stromatolite biostratigraphic evidence (Cloud & Dardenne 1973) for a late Mesoproterozoic age for the upper Vazante Group. In addition, Geboy (2006) has obtained Model 3 Re–Os ages of 1353 ± 69 Ma and 1126 ± 47 Ma for ORS from the upper Vazante Group. Thus, the upper Vazante Group glaciogenic diamictites are not correlative with 'Sturtian' (i.e. 750–643 Ma) glacial deposits, but instead may record a late Mesoproterozoic glaciation.

Timing of Earth surface oxygenation

Anbar *et al.* (2007) presented a high-resolution chemostratigraphic profile for the late Archaean Mt McRae Shale (Hamersley Basin, western Australia) that showed an episode of enrichment of the redox-sensitive metals Mo and Re in black shales. The suggested mechanism for metal enrichment was oxidative weathering and dissolution of Mo and Re derived from crustal sulphide minerals, transportation within or into an ocean basin, and sequestration into organic-rich sediments. A Re–Os depositional age of 2501.1 ± 8.2 Ma (Model 1, MSWD = 1.1) (Fig. 7c) agrees well with a U–Pb SHRIMP zircon age of 2504 ± 5 Ma (Rasmussen *et al.* 2005) from a tuffaceous bed within the Mt McRae Shale. Thus, the episode of metal enrichment is a primary sedimentary feature and suggests that shallow-water ocean oxygenation commenced more than 50 Ma prior to the Great Oxidation Event (2.45–2.32 Ga; Bekker *et al.* 2004). Thus, Re–Os ORS geochronology, together with geological and geochemical redox proxies, holds great potential for radiometrically constraining the timing of stepwise increases in atmosphere and ocean oxygen abundances during the Precambrian Eon.

Application to Precambrian petroleum systems

An example of a Precambrian ORS unit that has been studied for its petroleum source rock potential is the Mesoproterozoic Velkerri Formation (Roper Group, McArthur Basin, northern Australia). Within the Velkerri Formation there are three intervals, tens of metres thick, that are highly organic-rich (TOC >5%) and represent oil source beds (Jackson & Raiswell 1991; Warren *et al.* 1998). The world's oldest live oil is from the Velkerri Formation and has been observed bubbling from drillhole BMR Urapunga-4 at multiple depths (e.g. Jackson *et al.* 1986; Crick *et al.* 1988). Organic matter in the Velkerri Formation is mature, except where affected by a dolerite sill intrusion (Crick *et al.* 1988; Crick 1992; Summons *et al.* 1994; George & Ahmed 2002). During and prior to late Mesoproterozoic–early Neoproterozoic McArthur Basin inversion, the Velkerri Formation was the most likely source rock for multiple episodes of hydrocarbon migration into a cross-cutting dolerite sill and the overlying Bessie Creek Sandstone. The oldest known hydrocarbon migration event occurred prior to 1280 Ma (minimum K–Ar age of a dolerite sill: McDougall *et al.* 1965) and is associated with dolerite sill intrusion, which resulted in flash pyrolysis of kerogen and generation of bitumen. At least one younger hydrocarbon migration event is associated with basin inversion, and is represented by non-biodegraded fluid inclusion oils (Dutkiewicz *et al.* 2003, 2004; Volk *et al.* 2005).

Two Re–Os ages of 1361 ± 21 (Model 1, MSWD = 1.3) and 1417 ± 29 Ma (Model 1, MSWD = 1.3) were obtained by Kendall *et al.* (2009*a*) for the upper and lower organic-rich intervals of the Velkerri Formation, respectively (Fig. 7d). Both ages are internally consistent with stratigraphic position and with a U–Pb SHRIMP zircon age of 1492 ± 4 Ma from tuff within the Wooden Duck Member of the Mainoru Formation (>700 m beneath the Velkerri Formation: Jackson *et al.* 1999). Thus, the multiple hydrocarbon migration events do not appear to have affected the Re–Os systematics in the Velkerri Formation source rock, consistent with previous studies suggesting the Re–Os ORS geochronometer is robust up to the onset of greenschist facies metamorphism (Creaser *et al.* 2002; Kendall *et al.* 2004; Selby & Creaser 2005*a*). The Re–Os ages constrain the age of biomarkers in the Velkerri Formation and, together with the U–Pb zircon age of 1492 ± 4 Ma for the Mainoru Formation, suggest a duration of more than 100 Ma for the acritarch and microfossil record of the Roper Group (Javaux *et al.* 2001). In addition, the hydrocarbon migration event associated with the dolerite sill intrusion can be bracketed between the minimum K–Ar age of 1280 Ma and the Re–Os age of 1361 ± 21 Ma.

The Re–Os systematics of ORS source rocks are not grossly affected by hydrocarbon maturation, suggesting minimal fractionation of Re from Os during hydrocarbon generation and/or domination of the Re and Os mass balance by the source rock (Creaser *et al.* 2002). However, Selby & Creaser (2005*b*) and Selby *et al.* (2005) have shown that the Re–Os systematics of maturated hydrocarbons may be reset, possibly by some organic mechanism, during the process of hydrocarbon migration to the reservoir rock. In addition, Selby *et al.* (2007*a*) observed a strong correlation between the Os isotope composition of whole oils with source rock age. Thus, the Re–Os system in hydrocarbon deposits (e.g. bitumen, crude oil and oil sands) may constrain the timing of hydrocarbon migration

and entrapment, and serve as a tracer for fingerprinting hydrocarbon source rocks. We suggest that a joint application of the Re–Os system to Precambrian ORS source rocks and hydrocarbon deposits may ultimately prove valuable in understanding the age and nature of Precambrian petroleum systems. Such studies would complement more traditional organic geochemical methods such as source rock and hydrocarbon biomarker distributions, and thermal maturity indicators.

Summary and future directions

With rigorous sampling and analytical methodologies, we have shown that the ^{187}Re–^{187}Os isotope system represents a precise and accurate depositional-age geochronometer for ORS. However, we emphasize that some uncertainties still remain regarding the limitations of the Re–Os ORS geochronometer. For example, weathering (Peucker-Ehrenbrink & Hannigan 2000; Jaffe *et al.* 2002; Pierson-Wickmann *et al.* 2002) and hydrothermal fluid flow (Fig. 8) (Kendall *et al.* 2009*a*) are known to result in post-depositional mobilization of Re and Os. The robustness, or otherwise, of the Re–Os system in ORS at metamorphic grades above lowermost greenschist facies is not known. In addition, the mechanism controlling the range in initial ^{187}Re/^{188}Os of ORS is not fully understood, but may relate to the presence of multiple and/or separate organic complexes as host phases for Re and Os (Creaser *et al.* 2002; Selby & Creaser 2003). However, with further research, these questions should be resolved. If low abundances of Re in Archaean ORS are the norm (Yang & Holland 2002; Siebert *et al.* 2005; Wille *et al.* 2007), then the utility of Re–Os geochronology for ORS deposited prior to the Great Oxidation Event may be limited. Nevertheless, the Re–Os ORS geochronometer holds tremendous potential for constraining the rates, duration, timing and extent of geological phenomena during the Proterozoic Eon. Examples include timing of evolution and diversification of eukaryotes (including macroscopic metazoans), significant perturbations of biogeochemical cycles (e.g. positive and negative carbon isotope excursions), radiometric calibration of the Precambrian rock record and sedimentary basin analysis.

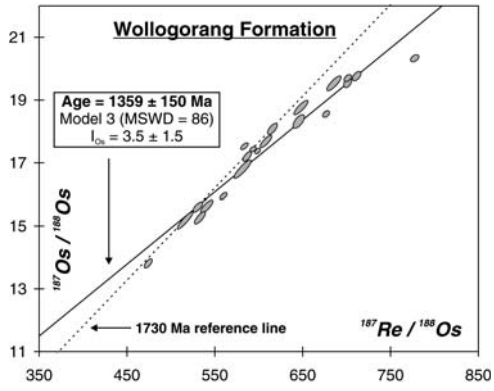

Fig. 8. Isochron diagram showing the scattered Re–Os isotope data for the Palaeoproterozoic Wollogorang Formation, McArthur Basin, northern Australia (Kendall *et al.* 2009*a*). The imprecise Re–Os date of 1359 ± 150 Ma is significantly younger than the U–Pb zircon ages of 1729 ± 4 and 1730 ± 3 Ma from tuffaceous beds within the Wollogorang Formation black shale unit that constrain the age of black shale deposition (Page *et al.* 2000). A *c.* 1730 Ma reference line (dashed line) with chondritic I_{Os} (0.115) is shown for comparison. Note the high I_{Os} value of 3.5 ± 1.5 from this regression that is significantly more radiogenic than currently eroding upper continental crust (e.g. ^{187}Os/^{188}Os *c.* 1.0–1.4: Esser & Turekian 1993; Peucker-Ehrenbrink & Jahn 2001; Hattori *et al.* 2003). Scattered Re–Os systematics are interpreted to result from post-depositional hydrothermal fluid flow, as evidenced by carbonate veinlets within the shale.

The constructive comments by G. Ravizza and A. Cohen improved the manuscript. This research was supported by a Natural Sciences and Engineering Research Council (NSERC) Discovery Grant to R. A. Creaser, and a NSERC Canada Graduate Scholarship, Alberta Ingenuity Fund PhD. Studentship and Geological Society of America Student Research Grant to B. Kendall. The Radiogenic Isotope Facility at the University of Alberta is supported in part by a NSERC Major Facilities Access Grant and Major Resources Support Grant. G. Jiang and M. Kennedy are thanked for Doushantuo Formation samples.

References

ANBAR, A. D., DUAN, Y. *ET AL*. 2007. A whiff of oxygen before the Great Oxidation Event. *Science*, **317**, 1903–1906.

ARTHUR, M. A. & SAGEMAN, B. B. 1994. Marine black shales: depositional mechanisms and environments of ancient deposits. *Annual Review of Earth and Planetary Science*, **22**, 499–551.

AZMY, K., KAUFMAN, A. J., MISI, A. & OLIVEIRA, T. F. 2006. Isotope stratigraphy of the Lapa Formation, São Francisco Basin, Brazil: implications for Late Neoproterozoic glacial events in South America. *Precambrian Research*, **149**, 231–248.

AZMY, K., KENDALL, B., CREASER, R. A., HEAMAN, L., MISI, A. & DE OLIVEIRA, T. F. 2008. Global correlation of the Vazante Group, São Francisco Basin, Brazil: Re–Os and U–Pb radiometric age constraints. *Precambrian Research*, **164**, 160–172.

AZMY, K., VEISER, J., MISI, A., OLIVEIRA, T. F., SANCHES, A. L. & DARDENNE, M. A. 2001.

Dolomitization and isotope stratigraphy of the Vazante Formation, São Francisco Basin, Brazil. *Precambrian Research*, **112**, 303–329.

BABINSKI, M., VIEIRA, L. C. & TRINDADE, R. I. F. 2007. Direct dating of the Sete Lagoas cap carbonate (Bambuí Group, Brazil) and implications for the Neoproterozoic glacial events. *Terra Nova*, **19**, 401–406.

BARFOD, G. H., ALBARÈDE, F., KNOLL, A. H., XIAO, S., TÉLOUK, P., FREI, R. & BAKER, J. 2002. New Lu–Hf and Pb–Pb age constraints on the earliest animal fossils. *Earth and Planetary Science Letters*, **201**, 203–212.

BARRE, A. B., PRINZHOFER, A. & ALLEGRE, C. J. 1995. Osmium isotopes in the organic matter of crude oil and asphaltenes. *Terra Abstracts*, **7**, 1999.

BECKER, H., MORGAN, J. W., WALKER, R. J., MACPHERSON, G. J. & GROSSMAN, J. N. 2001. Rhenium–osmium systematics of calcium–aluminum-rich inclusions in carbonaceous chondrites. *Geochimica et Cosmochimica Acta*, **65**, 3379–3390.

BEKKER, A. & HOLLAND, H. D. 2004. Dating the rise of atmospheric oxygen. *Nature*, **427**, 117–120.

BINGEN, B., GRIFFIN, W. L., TORSVIK, T. H. & SAEED, A. 2005. Timing of late Neoproterozoic glaciation on Baltica constrained by detrital zircon geochronology in the Hedmark Group, south-east Norway. *Terra Nova*, **17**, 250–258.

BIRCK, J.-L. & ALLÈGRE, C.-J. 1998. Rhenium 187–osmium 187 in iron meteorites and the strange origin of the Kodaikanal meteorite. *Meteoritic Planetary Science*, **33**, 647–653.

BRODY, K. B., KAUFMAN, A. J., EIGENBRODE, J. L. & CODY, G. D. 2004. Biomarker geochemistry of a post-glacial Neoproterozoic succession in Brazil. *Geological Society of America, Abstracts with Programs*, **36**(5), 477.

BURTON, K. W., BOURDON, B., BIRCK, J.-L., ALLÈGRE, C. J. & HEIN, J. R. 1999. Osmium isotope variations in the oceans recorded by Fe–Mn crusts. *Earth and Planetary Science Letters*, **171**, 185–197.

CANFIELD, D. E. 1998. A new model for Proterozoic ocean chemistry. *Nature*, **396**, 450–453.

CANFIELD, D. E., POULTON, S. W. & NARBONNE, G. M. 2007. Late-Neoproterozoic deep-ocean oxygenation and the rise of animal life. *Science*, **315**, 92–95.

CAVE, R. R., RAVIZZA, G. E., GERMAN, C. R., THOMSON, J. & NESBITT, R. W. 2003. Deposition of osmium and other platinum-group elements beneath the ultramafic-hosted Rainbow hydrothermal plume. *Earth and Planetary Science Letters*, **210**, 65–79.

CHEN, D. F., DONG, W. Q., ZHU, B. Q. & CHEN, X. P. 2004. Pb–Pb ages of Neoproterozoic Doushantuo phosphorites in South China: constraints on early metazoan evolution and glaciation events. *Precambrian Research*, **132**, 123–132.

CLOUD, P. E. & DARDENNE, M. A. 1973. Proterozoic age of the Bambuí Group in Brazil. *Geological Society of America Bulletin*, **84**, 1673–1676.

COHEN, A. S. 2004. The rhenium-osmium isotope system: applications to geochronological and palaeoenvironmental problems. *Journal of the Geological Society, London*, **161**, 729–734.

COHEN, A. S. & COE, A. L. 2002. New geochemical evidence for the onset of volcanism in the Central Atlantic magmatic province and environmental change at the Triassic–Jurassic boundary. *Geology*, **30**, 267–270.

COHEN, A. S. & COE, A. L. 2007. The impact of the Central Atlantic Magmatic Province on climate and on the Sr- and Os-isotope evolution of seawater. *Palaeogeography, Palaeoclimatology, Palaeoecology*, **244**, 374–390.

COHEN, A. S. & WATERS, F. G. 1996. Separation of osmium from geological materials by solvent extraction for analysis by thermal ionization mass spectrometry. *Analytical Chimica Acta*, **332**, 269–375.

COHEN, A. S., COE, A. L., BARTLETT, J. M. & HAWKESWORTH, C. J. 1999. Precise Re–Os ages of organic-rich mudrocks and the Os isotope composition of Jurassic seawater. *Earth and Planetary Science Letters*, **167**, 159–173.

COHEN, A. S., COE, A. L., HARDING, S. M. & SCHWARK, L. 2004. Osmium isotope evidence for the regulation of atmospheric CO_2 by continental weathering. *Geology*, **32**, 157–160.

COLODNER, D., SACHS, J., RAVIZZA, G., TUREKIAN, K., EDMOND, J. & BOYLE, E. 1993. The geochemical cycle of rhenium: a reconnaissance. *Earth and Planetary Science Letters*, **117**, 205–221.

COLPRON, M., LOGAN, J. M. & MORTENSEN, J. K. 2002. U–Pb zircon age constraint for late Neoproterozoic rifting and initiation of the lower Palaeozoic passive margin of western Laurentia. *Canadian Journal of Earth Sciences*, **39**, 133–143.

CONDON, D., ZHU, M., BOWRING, S., WANG, W., YANG, A. & JIN, Y. 2005. U–Pb ages from the Neoproterozoic Doushantuo Formation, China. *Science*, **308**, 95–98.

CREASER, R. A. & STASIUK, L. D. 2007. Depositional age of the Douglas Formation, northern Saskatchewan, determined by Re–Os geochronology. *In*: JEFFERSON, C. W. & DELANEY, G. (eds) *EXTECH IV: Geology and Uranium Exploration TECHnology of the Proterozoic Athabasca Basin, Saskatchewan and Alberta.* Geological Survey of Canada Bulletin, **588**, 341–346.

CREASER, R. A., PAPANASTASSIOU, D. A. & WASSERBURG, G. J. 1991. Negative thermal ion mass spectrometry of osmium, rhenium, and iridium. *Geochimica et Cosmochimica Acta*, **55**, 397–401.

CREASER, R. A., SANNIGRAHI, P., CHACKO, T. & SELBY, D. 2002. Further evaluation of the Re–Os geochronometer in organic-rich sedimentary rocks: a test of hydrocarbon maturation effects in the Exshaw Formation, Western Canada Sedimentary Basin. *Geochimica et Cosmochimica Acta*, **66**, 3441–3452.

CRICK, I. H. 1992. Petrological and maturation characteristics of organic matter from the Middle Proterozoic McArthur Basin, Australia. *Australian Journal of Earth Sciences*, **39**, 501–519.

CRICK, I. H., BOREHAM, C. J., COOK, A. C. & POWELL, T. G. 1988. Petroleum geology and geochemistry of Middle Proterozoic McArthur Basin, northern Australia II: Assessment of source rock potential. *AAPG Bulletin*, **72**, 1495–1514.

CRUSIUS, J. & THOMSON, J. 2000. Comparative behavior of authigenic Re, U, and Mo during reoxidation and subsequent long-term burial in marine sediments. *Geochimica et Cosmochimica Acta*, **64**, 2233–2242.

CRUSIUS, J., CALVERT, S., PEDERSEN, T. & SAGE, D. 1996. Rhenium and molybdenum enrichments in sediments as indicators of oxic, suboxic, and sulfidic conditions of deposition. *Earth and Planetary Science Letters*, **145**, 65–78.

DICKIN, A. P. 2005. *Radiogenic Isotope Geology*, 2nd edn. Cambridge University Press, Cambridge.

DUTKIEWICZ, A., VOLK, H., RIDLEY, J. & GEORGE, S. 2003. Biomarkers, brines, and oil in the Mesoproterozoic, Roper Superbasin, Australia. *Geology*, **31**, 981–984.

DUTKIEWICZ, A., VOLK, H., RIDLEY, J. & GEORGE, S. C. 2004. Geochemistry of oil in fluid inclusions in a middle Proterozoic igneous intrusion: implications for the source of hydrocarbons in crystalline rocks. *Organic Geochemistry*, **35**, 937–957.

ENGLAND, G. L., RASMUSSEN, B., KRAPEZ, B. & GROVES, D. I. 2002. Palaeoenvironmental significance of rounded pyrite in siliciclastic sequences of the Late Archaean Witwatersrand Basin: oxygen-deficient atmosphere or hydrothermal alteration? *Sedimentology*, **49**, 1133–1156.

ESSER, B. K. & TUREKIAN, K. K. 1993. The osmium isotopic composition of the continental crust. *Geochimica et Cosmochimica Acta*, **57**, 3093–3104.

FARQUHAR, J. & WING, B. A. 2003. Multiple sulfur isotopes and the evolution of the atmosphere. *Earth and Planetary Science Letters*, **213**, 1–13.

FARQUHAR, J., BAO, H. & THIEMENS, M. 2000. Atmospheric influence of Earth's earliest sulfur cycle. *Science*, **289**, 756–758.

FANNING, C. M. & LINK, P. K. 2004. U–Pb SHRIMP ages of Neoproterozoic (Sturtian) glaciogenic Pocatello Formation, southeastern Idaho. *Geology*, **32**, 881–884.

FANNING, C. M. & LINK, P. K. 2008. Age constraints for the Sturtian glaciation: data from the Adelaide Geosyncline, South Australia and Pocatello Formation, Idaho, USA. *In*: GALLAGHER, S. J. & WALLACE, M. W. (eds) *Neoproterozoic Extreme Climates and the Origin of Early Life*, Selwyn Symposium of the GSA Victoria Division. Geological Society of Australia Extended Abstracts, **91**, 57–62.

FIKE, D. A., GROTZINGER, J. P., PRATT, L. M. & SUMMONS, R. E. 2006. Oxidation of the Ediacaran ocean. *Nature*, **444**, 744–747.

FLEET, M. E. 1998. Detrital pyrite in Witwatersrand gold reefs: X-ray diffraction evidence and implications for atmospheric evolution. *Terra Nova*, **10**, 302–306.

GEBOY, N. J. 2006. *Rhenium-osmium age determinations of glaciogenic shales, Vazante Formation, Brazil*. Unpublished M.Sc. Thesis, University of Maryland, College Park.

GEORGE, S. C. & AHMED, M. 2002. Use of aromatic compound distributions to evaluate organic maturity of the Proterozoic Middle Velkerri Formation, McArthur Basin, Australia. *In*: KEEP, M. & MOSS, S. J. (eds) *The Sedimentary Basins of Western Australia, 3.* Proceedings of the Petroleum Exploration Society of Australia Symposium, 253–270.

GOLDBLATT, C., LENTON, T. M. & WATSON, A. J. 2006. Bistability of atmospheric oxygen and the Great Oxidation. *Nature*, **443**, 683–686.

GRADSTEIN, F. M., OGG, J. G. & SMITH, A. G. 2004. *A Geologic Time Scale 2004.* Cambridge University Press, Cambridge.

HALVERSON, G. P., HOFFMAN, P. F., SCHRAG, D. P., MALOOF, A. C. & RICE, A. H. N. 2005. Toward a Neoproterozoic composite carbon-isotope record. *Geological Society of America Bulletin*, **117**, 1181–1207.

HANNAH, J. L., BEKKER, A., STEIN, H. J., MARKEY, R. J. & HOLLAND, H. D. 2004. Primitive Os and 2316 Ma age for marine shale: implications for Palaeoproterozoic glacial events and the rise of atmospheric oxygen. *Earth and Planetary Science Letters*, **225**, 43–52.

HANNAH, J. L., STEIN, H. J., ZIMMERMAN, A., YANG, G., MARKEY, R. J. & MELEZHIK, V. A. 2006. Precise 2004 $\pm$ 9 Ma Re–Os age for Pechenga black shale: comparison of sulfides and organic material. *Geochimica et Cosmochimica Acta*, **70**(18; Supplement 1), A228.

HATTORI, Y., SUZUKI, K., HONDA, M. & SHIMIZU, H. 2003. Re–Os isotope systematics of the Taklimakan Desert sands, moraines and river sediments around the Taklimakan Desert, and of Tibetan soils. *Geochimica et Cosmochimica Acta*, **67**, 1195–1205.

HEIN, F. J. & MCMECHAN, M. E. 1994. Proterozoic–Lower Cambrian strata of the Western Canada Sedimentary Basin. *In*: MOSSOP, G. D. & SHETSEN, I. (eds) *Geological Atlas of the Western Canada Sedimentary Basin.* Canadian Society of Petroleum Geologists, Calgary, Alberta, 57–68.

HOFFMAN, P. F., HAWKINS, D. P., ISACHSEN, C. E. & BOWRING, S. A. 1996. Precise U–Pb zircon ages for early Damaran magmatism in the Summas Mountains and Welwitschia Inlier, northern Damara Belt, Namibia. *Communications of the Geological Survey of Namibia*, **11**, 47–52.

HOFFMANN, K.-H., CONDON, D. J., BOWRING, S. A. & CROWLEY, J. L. 2004. U–Pb zircon date from the Neoproterozoic Ghaub Formation, Namibia: constraints on Marinoan glaciation. *Geology*, **32**, 817–820.

HUTCHEON, I. D. & OLSEN, E. 1991. Cr isotopic composition of differentiated meteorites: A search for ^{53}Mn. *Lunar and Planetary Sciences*, **22**, 605–606.

HUTCHEON, I. D., OLSEN, E., ZIPFEL, J. & WASSERBURG, G. J. 1992. Cr isotopic composition of differentiated meteorites: Evidence for ^{53}Mn. *Lunar and Planetary Sciences*, **23**, 565–566.

JACKSON, M. J. & RAISWELL, R. 1991. Sedimentology and carbon–sulphur geochemistry of the Velkerri Formation, a Mid-Proterozoic potential oil source in northern Australia. *Precambrian Research*, **54**, 81–108.

JACKSON, M. J., POWELL, T. G., SUMMONS, R. E. & SWEET, I. P. 1986. Hydrocarbon shows and petroleum source rocks in sediments as old as 1.7×10^9 years. *Nature*, **322**, 727–729.

JACKSON, M. J., SWEET, I. P., PAGE, R. W. & BRADSHAW, B. E. 1999. The South Nicholson and Roper Groups: evidence for the early Mesoproterozoic Roper Superbasin. *In*: *Integrated Basin Analysis of the Isa Superbasin using Seismic, Well-log, and*

Geopotential Data: An Evaluation of the Economic Potential of the Northern Lawn Hill Platform. Australian Geological Survey Organisation Record 1999/19 (unpaginated).

JAFFE, L. A., PEUCKER-EHRENBRINK, B. & PETSCH, S. T. 2002. Mobility of rhenium, platinum group elements and organic carbon during black shale weathering. *Earth and Planetary Science Letters*, **198**, 339–353.

JAFFEY, A. H., FLYNN, K. F., GLENDENIN, L. E., BENTLEY, W. C. & ESSLING, A. M. 1971. Precision measurement of half-lives and specific activities of ^{235}U and ^{238}U. *Physics Reviews*, **4**, 1889–1906.

JAVAUX, E. J., KNOLL, A. H. & WALTER, M. R. 2001. Morphological and ecological complexity in early eukaryotic ecosystems. *Nature*, **412**, 66–69.

JIANG, G., SOHL, L. E. & CHRISTIE-BLICK, N. 2003. Neoproterozoic stratigraphic comparison of the Lesser Himalaya (India) and Yangtze block (south China): palaeogeographic implications. *Geology*, **31**, 917–920.

KENDALL, B. S., CREASER, R. A., ROSS, G. M. & SELBY, D. 2004. Constraints on the timing of Marinoan 'Snowball Earth' glaciation by ^{187}Re–^{187}Os dating of a Neoproterozoic, post-glacial black shale in Western Canada. *Earth and Planetary Science Letters*, **222**, 729–740.

KENDALL, B., CREASER, R. A. & SELBY, D. 2006. Re–Os geochronology of postglacial black shales in Australia: constraints on the timing of 'Sturtian' glaciation. *Geology*, **34**, 729–732.

KENDALL, B., CREASER, R. A., GORDON, G. W. & ANBAR, A. D. 2009*a*. Re–Os and Mo isotope systematics of black shales from the Middle Proterozoic Velkerri and Wollogorang Formations, McArthur Basin, northern Australia. *Geochimica et Cosmochimica Acta*, **73**, 2534–2558.

KENDALL, B., CREASER, R. A., CALVER, C. R., RAUB, T. D. & EVANS, D. A. D. 2009*b*. Correlation of Sturtian diamictite successions in southern Australia and northwestern Tasmania by Re–Os black shale geochronology and the ambiguity of "Sturtian"-type diamictite-cap carbonate pairs as chronostratigraphic marker horizons. *Precambrian Research*, **172**, 301–310.

KENNEDY, M., DROSER, M., MAYER, L. M., PEVEAR, D. & MROFKA, D. 2006. Late Precambrian oxygenation; inception of the clay mineral factory. *Science*, **311**, 1446–1449.

KENNEDY, M. J., RUNNEGAR, B., PRAVE, A. R., HOFFMANN, K.-H. & ARTHUR, M. A. 1998. Two or four Neoproterozoic glaciations? *Geology*, **26**, 1059–1063.

LEVASSEUR, S., BIRCK, J.-L. & ALLÈGRE, C. J. 1998. Direct measurement of femtomoles of osmium and the $^{187}Os/^{186}Os$ ratio in seawater. *Science*, **282**, 272–274.

LEVASSEUR, S., BIRCK, J.-L. & ALLÈGRE, C. J. 1999. The osmium riverine flux and the oceanic mass balance of osmium. *Earth and Planetary Science Letters*, **174**, 7–23.

LOTTAROLI, F., CRAIG, J. & THUSU, B. 2009. Neoproterozoic–Early Cambrian (Infracambrian) hydrocarbon prospectivity of North Africa: a synthesis. *In*: CRAIG, J., THUROW, J., THUSU, B., WHITHAM, A. & ABUTARRUMA, Y. (eds) *Global Neoproterozoic Petroleum Systems: The Emerging Potential in North Africa*. Geological Society, London, Special Publications, **326**, 137–156.

LUCK, J.-M. & ALLÈGRE, C. J. 1983. ^{187}Re–^{187}Os systematics in meteorites and cosmochemical consequences. *Nature*, **302**, 130–132.

LUDWIG, K. 1980. Calculation of uncertainties of U–Pb isotope data. *Earth and Planetary Science Letters*, **46**, 212–220.

LUDWIG, K. 2003. *Isoplot/Ex, Version 3: A Geochronological Toolkit for Microsoft Excel*. Berkely Geochronology Center, Berkeley, CA.

LUGMAIR, G. W. & GALER, S. J. G. 1992. Age and isotopic relationships among angrites Lewis Cliff 86010 and Angra dos Reis. *Geochimica et Cosmochimica Acta*, **56**, 1673–1694.

LUND, K., ALEINIKOFF, J. N., EVANS, K. V. & FANNING, C. M. 2003. SHRIMP U–Pb geochronology of Neoproterozoic Windermere Supergroup, central Idaho: Implications for rifting of western Laurentia and synchroneity of Sturtian glacial deposits. *Geological Society of America Bulletin*, **115**, 349–372.

MARTIN, C. E., PEUCKER-EHRENBRINK, B., BRUNSKILL, G. J. & SZYMCZAK, R. 2000. Sources and sinks of unradiogenic osmium runoff from Papua New Guinea. *Earth and Planetary Science Letters*, **183**, 261–274.

MCDANIEL, D. K., WALKER, R. J., HEMMING, S. R., HORAN, M. F., BECKER, H. & GRAUCH, R. I. 2004. Sources of osmium to the modern oceans: new evidence from the ^{190}Pt–^{186}Os system. *Geochimica et Cosmochimica Acta*, **68**, 1243–1252.

MCDOUGALL, I., DUNN, P. R., COMPSTON, W., WEBB, A. W., RICHARDS, J. R. & BOFINGER, V. M. 1965. Isotopic age determinations on Precambrian rocks of the Carpentaria region, Northern Territory, Australia. *Journal of the Geological Society of Australia*, **12**, 67–90.

MCMECHAN, M. E. 2000. Vreeland diamictites – Neoproterozoic glaciogenic slope deposits, Rocky Mountains, northeast British Columbia. *Bulletin of Canadian Petroleum Geology*, **48**, 246–261.

MEISEL, T., WALKER, R. J., IRVING, A. J. & LORAND, J.-P. 2001. Osmium isotopic compositions of mantle xenoliths: a global perspective. *Geochimica et Cosmochimica Acta*, **65**, 1311–1323.

MEISEL, T., WALKER, R. J. & MORGAN, J. W. 1996. The osmium isotopic composition of the Earth's primitive upper mantle. *Nature*, **383**, 517–520.

MOORBATH, S., TAYLOR, P. N., ORPEN, J. L., TRELOAR, P. & WILSON, J. F. 1987. First direct radiometric dating of Archaean stromatolitic limestone. *Nature*, **326**, 865–867.

MORFORD, J. L. & EMERSON, S. 1999. The geochemistry of redox sensitive trace metals in sediments. *Geochimica et Cosmochimica Acta*, **63**, 1735–1750.

MORFORD, J. L., EMERSON, S. R., BRECKEL, E. J. & KIM, S. H. 2005. Diagenesis of oxyanions (V, U, Re, and Mo) in pore waters and sediments from a continental margin. *Geochimica et Cosmochimica Acta*, **69**, 5021–5032.

MORGAN, J. W., HORAN, M. F., WALKER, R. J. & GROSSMAN, J. N. 1995. Rhenium–osmium concentration and isotope systematics in group IIAB iron

meteorites. *Geochimica et Cosmochimica Acta*, **59**, 2331–2344.

NAMEROFF, T. J., BALISTRIERI, L. S. & MURRAY, J. W. 2002. Suboxic trace metal geochemistry in the eastern tropical North Pacific. *Geochimica et Cosmochimica Acta*, **66**, 1139–1158.

NARBONNE, G. M. & AITKEN, J. D. 1995. Neoproterozoic of the Mackenzie Mountains, northwestern Canada. *Precambrian Research*, **73**, 101–121.

OLCOTT, A. N., SESSIONS, A. L., CORSETTI, F. A., KAUFMAN, A. J. & OLIVIERA, T. F. 2005. Biomarker evidence for photosynthesis during Neoproterozoic glaciation. *Science*, **310**, 471–474.

OXBURGH, R. 1998. Variations in the osmium isotope composition of seawater over the past 200,000 years. *Earth and Planetary Science Letters*, **159**, 183–191.

OXBURGH, R. 2001. Residence time of osmium in the oceans. *Geochemistry, Geophysics, Geosystems*, **2**(6), 1018.

PAGE, R. W., JACKSON, M. J. & KRASSAY, A. A. 2000. Constraining sequence stratigraphy in north Australian basins: SHRIMP U–Pb zircon geochronology between Mt Isa and McArthur River. *Australian Journal of Earth Sciences*, **47**, 431–459.

PAVLOV, A. A. & KASTING, J. F. 2002. Mass-independent fractionation of sulfur isotopes in Archean sediments: strong evidence for an anoxic Archean atmosphere. *Astrobiology*, **2**, 27–41.

PEGRAM, W. J. & TUREKIAN, K. K. 1999. The osmium isotopic composition change of Cenozoic sea water as inferred from a deep-sea core corrected for meteoritic contributions. *Geochimica et Cosmochimica Acta*, **63**, 4053–4058.

PETERS, K. E., WALTERS, C. C. & MOLDOWAN, J. M. 2005. Petroleum systems through time, Chapter 18. *In*: *The Biomarker Guide, Volume 2: Biomarkers and Isotopes in Petroleum Exploration and Earth History*, 2nd edn. Cambridge University Press, Cambridge, 751–964.

PEUCKER-EHRENBRINK, B. 1996. Accretion of extraterrestrial matter during the last 80 million years and its effect on the marine osmium isotope record. *Geochimica et Cosmochimica Acta*, **60**, 3187–3196.

PEUCKER-EHRENBRINK, B. & HANNIGAN, R. E. 2000. Effects of black shale weathering on the mobility of rhenium and platinum group elements. *Geology*, **28**, 475–478.

PEUCKER-EHRENBRINK, B. & JAHN, B.-M. 2001. Rhenium–osmium isotope systematics and platinum group element concentrations: Loess and the upper continental crust. *Geochemistry Geophysics Geosystems*, **2**(10), 1061.

PEUCKER-EHRENBRINK, B. & RAVIZZA, G. 2000. The marine osmium isotope record. *Terra Nova*, **12**, 205–219.

PEUCKER-EHRENBRINK, B., RAVIZZA, G. & HOFMANN, A. W. 1995. The marine $^{187}Os/^{186}Os$ record of the past 80 million years. *Earth and Planetary Science Letters*, **130**, 155–167.

PIERSON-WICKMANN, A.-C., REISBERG, L. & FRANCE-LANORD, C. 2000. The Os isotopic composition of Himalayan river bedloads and bedrocks: importance of black shales. *Earth and Planetary Science Letters*, **176**, 203–218.

PIERSON-WICKMANN, A.-C., REISBERG, L. & FRANCE-LANORD, C. 2002. Behavior of Re and Os during low-temperature alteration: results from Himalayan soils and altered black shales. *Geochimica et Cosmochimica Acta*, **66**, 1539–1548.

POIRIER, A. 2006. Re–Os and Pb isotope systematics in reduced fjord sediments from Saanich Inlet (Western Canada). *Earth and Planetary Science Letters*, **249**, 119–131.

POPLAVKO, Y. M., IVANOV, V. V. *ET AL.* 1975. On the concentration of rhenium in petroleum, petroleum bitumens and oil shales. *Geochemistry International*, **11**, 969–972.

PREISS, W. V. 2000. The Adelaide Geosyncline of south Australia and its significance in Neoproterozoic continental reconstruction. *Precambrian Research*, **100**, 21–63.

RASMUSSEN, B. 2005. Radiometric dating of sedimentary rocks: the application of diagenetic xenotime geochronology. *Earth-Science Reviews*, **68**, 197–243.

RASMUSSEN, B. & BUICK, R. 1999. Redox state of the Archean atmosphere: evidence from detrital heavy minerals in ca. 3250–2750 Ma sandstones from the Pilbara Craton, Australia. *Geology*, **27**, 115–118.

RASMUSSEN, B., BLAKE, T. S. & FLETCHER, I. R. 2005. U–Pb zircon age constraints on the Hamersley spherule beds: Evidence for a single 2.63 Ga Jeerinah–Carawine impact ejecta layer. *Geology*, **33**, 725–728.

RAVIZZA, G. & ESSER, B. K. 1993. A possible link between the seawater osmium isotope record and weathering of ancient sedimentary organic matter. *Chemical Geology*, **107**, 255–258.

RAVIZZA, G. & PAQUAY, F. 2008. Os isotope chemostratigraphy applied to organic-rich marine sediments from the Eocene–Oligocene transition on the West African margin (ODP Site 959). *Palaeoceanography*, **23**, PA2204, doi:10.1029/2007PA001460.

RAVIZZA, G. & PEUCKER-EHRENBRINK, B. 2003. Chemostratigraphic evidence of Deccan volcanism from the marine osmium isotope record. *Science*, **302**, 1392–1395.

RAVIZZA, G. & TUREKIAN, K. K. 1989. Application of the $^{187}Re-^{187}Os$ system to black shale geochronometry. *Geochimica et Cosmochimica Acta*, **53**, 3257–3262.

RAVIZZA, G. & TUREKIAN, K. K. 1992. The osmium isotopic composition of organic-rich marine sediments. *Earth and Planetary Science Letters*, **110**, 1–6.

RAVIZZA, G., MARTIN, C. E., GERMAN, C. R. & THOMPSON, G. 1996. Os isotopes as tracers in seafloor hydrothermal systems: metalliferous deposits from the TAG hydrothermal area, 26°N Mid-Atlantic Ridge. *Earth and Planetary Science Letters*, **138**, 105–119.

RAVIZZA, G., NORRIS, R. N., BLUSZTAJN, J. & AUBRY, M. P. 2001. An osmium isotope excursion associated with the late Palaeocene thermal maximum: evidence of intensified chemical weathering. *Palaeoceanography*, **16**, 155–163.

RAVIZZA, G., TUREKIAN, K. K. & HAY, B. J. 1991. The geochemistry of rhenium and osmium in recent sediments from the Black Sea. *Geochimica et Cosmochimica Acta*, **55**, 3741–3752.

RICHARDS, B. C., ROSS, G. M. & UTTING, J. 2002. U–Pb geochronology, lithostratigraphy and biostratigraphy of tuff in the upper Famennian to Tournaisian Exshaw Formation: Evidence for a mid-Palaeozoic magmatic arc on the northwestern margin of North America. *In*: HILLS, L. V., HENDRSON, C. M. & BAMBER, E. W. (eds) *Carboniferous and Permian of the World: XIV ICCP Proceedings*. Canadian Society of Petroleum Geologists Memoir, **19**, 158–207.

RIPLEY, E. M., PARK, Y.-R., LAMBERT, D. D. & FRICK, L. R. 2001. Re–Os isotopic composition and PGE contents of Proterozoic carbonaceous argillites, Virginia Formation, Northeastern Minnesota. *Organic Geochemistry*, **32**, 857–866.

ROSS, G. M., BLOCH, J. D. & KROUSE, H. R. 1995. Neoproterozoic strata of the southern Canadian Cordillera and the isotopic evolution of seawater sulfate. *Precambrian Research*, **73**, 71–99.

SCHAEFER, B. F. & BURGESS, J. M. 2003. Re–Os isotopic age constraints on deposition in the Neoproterozoic Amadeus Basin: implications for the 'Snowball Earth'. *Journal of the Geological Society, London*, **160**, 825–828.

SCHOENE, B., CROWLEY, J. L., CONDON, D. J., SCHMITZ, M. D. & BOWRING, S. A. 2006. Reassessing the uranium decay constants for geochronology using ID-TIMS U–Pb data. *Geochimica et Cosmochimica Acta*, **70**, 426–445.

SELBY, D. 2007. Direct rhenium–osmium age of the Oxfordian–Kimmeridgian boundary, Staffin Bay, Isle of Skye, UK, and the Late Jurassic time scale. *Norwegian Journal of Geology*, **87**, 291–299.

SELBY, D. & CREASER, R. A. 2001. Re–Os geochronology and systematics in molybdenite from the Endako porphyry molybdenum deposit, British Columbia, Canada. *Economic Geology*, **96**, 197–204.

SELBY, D. & CREASER, R. A. 2003. Re–Os geochronology of organic-rich sediments: an evaluation of organic matter analysis methods. *Chemical Geology*, **200**, 225–240.

SELBY, D. & CREASER, R. A. 2004. Macroscale NTIMS and microscale LA-MC-ICP-MS Re–Os isotopic analysis of molybdenite: testing spatial restrictions for reliable Re–Os age determinations, and implications for the decoupling of Re and Os within molybdenite. *Geochimica et Cosmochimica Acta*, **68**, 3897–3908.

SELBY, D. & CREASER, R. A. 2005*a*. Direct radiometric dating of the Devonian–Mississippian time-scale boundary using the Re–Os black shale geochronometer. *Geology*, **33**, 545–548.

SELBY, D. & CREASER, R. A. 2005*b*. Direct radiometric dating of hydrocarbon deposits using rhenium–osmium isotopes. *Science*, **308**, 1293–1295.

SELBY, D., CREASER, R. A., DEWING, K. & FOWLER, M. 2005. Evaluation of bitumen as a ^{187}Re–^{187}Os geochronometer for hydrocarbon maturation and migration: a case study from the Polaris MVT deposit, Canada. *Earth and Planetary Science Letters*, **235**, 1–15.

SELBY, D., CREASER, R. A. & FOWLER, M. G. 2007*a*. Re–Os elemental and isotopic systematics in crude oils. *Geochimica et Cosmochimica Acta*, **71**, 378–386.

SELBY, D., CREASER, R. A., STEIN, H. J., MARKEY, R. J. & HANNAH, J. L. 2007*b*. Assessment of the ^{187}Re decay constant by cross calibration of Re–Os molybdenite and U–Pb zircon chronometres in magmatic ore systems. *Geochimica et Cosmochimica Acta*, **71**, 1999–2013.

SHARMA, M., PAPANASTASSIOU, D. A. & WASSERBURG, G. J. 1997. The concentration and isotopic composition of osmium in the oceans. *Geochimica et Cosmochimica Acta*, **61**, 3287–3299.

SHARMA, M., ROSENBERG, E. J. & BUTTERFIELD, D. A. 2007. Search for the proverbial mantle osmium sources to the oceans: hydrothermal alteration of mid-ocean ridge basalt. *Geochimica et Cosmochimica Acta*, **71**, 4655–4667.

SHARMA, M., WASSERBURG, G. J., HOFMANN, A. W. & BUTTERFIELD, D. A. 2000. Osmium isotopes in hydrothermal fluids from the Juan de Fuca Ridge. *Earth and Planetary Science Letters*, **179**, 139–152.

SHEN, J. J., PAPANASTASSIOU, D. A. & WASSERBURG, G. J. 1998. Re–Os systematics in pallasite and mesosiderite metal. *Geochimica et Cosmochimica Acta*, **62**, 2715–2723.

SHIREY, S. B. & WALKER, R. J. 1995. Carius tube digestion for low-blank rhenium–osmium analysis. *Analytical Chemistry*, **67**, 2136–2141.

SHIREY, S. B. & WALKER, R. J. 1998. The Re–Os isotope system in cosmochemistry and high temperature geochemistry. *Annual Reviews of Earth and Planetary Sciences*, **26**, 423–500.

SHUKOLYUKOV, A. & LUGMAIR, G. W. 1997. The ^{53}Mn–^{53}Cr isotope system in the Omolon pallasite and the half-life of ^{187}Re. *Lunar and Planetary Sciences Abstracts*, **28**, 1315–1316.

SIEBERT, C., KRAMERS, J. D., MEISEL, T., MOREL, P. & NÄGLER, T. F. 2005. PGE, Re–Os, and Mo isotope systematics in Archean and early Proterozoic sedimentary systems as proxies for redox conditions of the early Earth. *Geochimica et Cosmochimica Acta*, **69**, 1787–1801.

SLACK, J. F., GRENNE, T., BEKKER, A., ROUXEL, O. J. & LINDBERG, P. A. 2007. Suboxic deep seawater in the late Palaeoproterozoic: evidence from hematitic chert and iron formation related to seafloor-hydrothermal sulfide deposits, central Arizona, USA. *Earth and Planetary Science Letters*, **255**, 243–256.

SMOLIAR, M. I., WALKER, R. J. & MORGAN, J. W. 1996. Re–Os ages of Group IIA, IIIA, IVA, and IVB iron meteorites. *Science*, **271**, 1099–1102.

SUMMONS, R. E., TAYLOR, D. & BOREHAM, C. J. 1994. Geochemical tools for evaluating petroleum generation in Middle Proterozoic sediments of the McArthur Basin, Northern Territory, Australia. *Australian Petroleum Exploration Association Journal*, **34**, 692–706.

SUN, W., ARCULUS, R. J., BENNETT, V. C., EGGINS, S. M. & BINNS, R. A. 2003*a*. Evidence for rhenium enrichment in the mantle wedge from submarine arc-like volcanic glasses (Papua New Guinea). *Geology*, **31**, 845–848.

SUN, W., BENNETT, V. C., EGGINS, S. M., KAMENETSKY, V. S. & ARCULUS, R. J. 2003*b*. Enhanced mantle-to-crust rhenium transfer in undegassed arc magmas. *Nature*, **422**, 294–297.

SUNDBY, B., MARTINEZ, P. & GOBEIL, C. 2004. Comparative geochemistry of cadmium, rhenium, uranium, and molybdenum in continental margin sediments. *Geochimica et Cosmochimica Acta*, **68**, 2485–2493.

TRAPP, E., KAUFMANN, B., MEZGER, K., KORN, M. & WEYER, D. 2004. Numerical calibration of the Devonian–Mississippian boundary: Two new U–Pb isotope dilution-thermal ionization mass spectrometry single-zircon ages from Hasselbachtal (Sauerland, Germany). *Geology*, **32**, 857–860.

VOLK, H., GEORGE, S. C., DUTKIEWICZ, A. & RIDLEY, J. 2005. Characterisation of fluid inclusion oil in a Mid-Proterozoic sandstone and dolerite (Roper Superbasin, Australia). *Chemical Geology*, **223**, 109–135.

VÖLKENING, J., WALCZYK, T. & HEUMANN, K. G. 1991. Osmium isotope ratio determinations by negative thermal ionization mass spectrometry. *International Journal of Mass Spectrometry and Ion Processes*, **105**, 147–159.

WALCZYK, T., HEBEDA, E. H. & HEUMANN, K. G. 1991. Osmium isotope ratio measurements by negative thermal ionization mass spectrometry (NTI-MS): Improvement in precision and enhancement in emission by introducing oxygen or Freon into the ion source. *Fresenius' Journal of Analytical Chemistry*, **341**, 537–541.

WALKER, R. J., HORAN, M. F., MORGAN, J. W., BECKER, H., GROSSMAN, J. N. & RUBIN, A. E. 2002*a*. Comparative $^{187}Re-^{187}Os$ systematics of chondrites: implications regarding early solar system processes. *Geochimica et Cosmochimica Acta*, **66**, 4187–4201.

WALKER, R. J., PRICHARD, H. M., ISHIWATARI, A. & PIMENTEL, M. 2002*b*. The osmium isotopic composition of convecting upper mantle deduced from ophiolite chromites. *Geochimica et Cosmochimica Acta*, **66**, 329–345.

WALTER, M. R., VEEVERS, J. J., CALVER, C. R., GORJAN, P. & HILL, A. C. 2000. Dating the 840–544 Ma Neoproterozoic interval by isotopes of strontium, carbon, and sulfur in seawater, and some interpretative models. *Precambrian Research*, **100**, 371–433.

WANG, X., ERDTMANN, B.-D., CHEN, X. & MAO, X. 1998. Integrated sequence-, bio- and chemo-stratigraphy of the terminal Proterozoic to lowermost Cambrian 'black rock series' from central South China. *Episodes*, **21**, 178–189.

WARREN, J. K., GEORGE, S. C., HAMILTON, P. J. & TINGATE, P. 1998. Proterozoic source rocks: sedimentology and organic characteristics of the Velkerri Formation, Northern Territory, Australia. *AAPG Bulletin*, **82**, 442–463.

WILLE, M., KRAMERS, J. D. *ET AL*. 2007. Evidence for a gradual rise of oxygen between 2.6 and 2.5 Ga from Mo isotopes and Re-PGE signatures in shales. *Geochimica et Cosmochimica Acta*, **71**, 2417–2435.

WOODHEAD, J. D., HERGT, J. M. & SIMONSON, B. M. 1998. Isotopic dating of an Archean bolide impact horizon, Hamersley Basin, Western Australia. *Geology*, **26**, 47–50.

WOODHOUSE, O. B., RAVIZZA, G., FALKNER, K. K., STATHAM, P. J. & PEUCKER-EHRENBRINK, B. 1999. Osmium in seawater: vertical profiles of concentration and isotopic composition in the eastern Pacific Ocean. *Earth and Planetary Science Letters*, **173**, 223–233.

WOODLAND, S. J., OTTLEY, C. J., PEARSON, D. G. & SWARBRICK, R. E. 2001. Microwave digestion of oils for analysis of platinum group and rare earth elements by ICP-MS. *In*: HOLLAND, G. & BANDURA, D. (eds) *Plasma Source Mass Spectrometry. Current Trends and Future Developments*. Royal Society of Chemistry, Special Publications, **301**, 17–24.

XIAO, S., YUAN, X., STEINER, M. & KNOLL, A. H. 2002. Macroscopic carbonaceous compressions in a terminal Proterozoic shale: a systematic reassessment of the Miaohe biota, South China. *Journal of Palaeontology*, **76**, 347–376.

XIAO, S., ZHANG, Y. & KNOLL, A. H. 1998. Three-dimensional preservation of algae and animal embryos in a Neoproterozoic phosphorite. *Nature*, **391**, 553–558.

YAMASHITA, Y., TAKAHASHI, Y., HABA, H., ENOMOTO, S. & SHIMIZU, H. 2007. Comparison of reductive accumulation of Re and Os in seawater–sediment systems. *Geochimica et Cosmochimica Acta*, **71**, 3458–3475.

YANG, W. & HOLLAND, H. D. 2002. The redox-sensitive trace elements, Mo, U, and Re in Precambrian carbonaceous shales: indicators of the Great Oxidation Event. *Geological Society of America, Abstracts with Programs*, **34**, 381.

YANG, G., HANNAH, J. L., ZIMMERMAN, A., STEIN, H. J. & BEKKER, A. 2009. Re–Os depositional age for Archean carbonaceous slates from the southwestern Superior Province: challenges and insights. *Earth and Planetary Science Letters*, **280**, 83–92.

ZHOU, C. & XIAO, S. 2007. Ediacaran $\delta^{13}C$ chemostratigraphy of South China. *Chemical Geology*, **237**, 89–108.